ARTICLE IN PRESS

+ MODEL

Available online at www.sciencedirect.com

SCIENCE DIRECT®

Gondwana Research xx (2006) xxx – xxx

www.elsevier.com/locate/gr

The Mesoarchean emergence of modern-style subduction

R.H. Smithies [a,*], M.J. Van Kranendonk [a], D.C. Champion [b]

[a] Geological Survey of Western Australia, 100 Plain Street East Perth, WA 6004, Australia

[b] Geoscience Australia, GPO Box 378, Canberra, ACT 2601, Australia

Received 12 December 2005; received in revised form 2 February 2006; accepted 2 February 2006

Abstract

Well-preserved volcanic sequences span the Paleoarchean to Neoarchean evolution of the Pilbara Craton, in northwestern Australia. This region provides the best physical evidence bearing on the stage of Earth's history when modern-style tectonic processes began. Paleoarchean assemblages in the eastern nucleus of the craton (the 3.51–3.24 Ga Pilbara Supergroup) show few features that can reasonably be interpreted as evidence for modern-style subduction processes. Incompatible trace element-enriched felsic volcanic horizons show geochemical evidence for the interaction between mafic magmas and crust, but this evidence, on its own, can equally well be interpreted in terms of either a subduction-enriched mantle source or local and limited assimilation of felsic crust into the voluminous tholeiitic magmas that dominate the Pilbara Supergroup. Viewed in context within the thick autochthonous and consistently upward-younging Pilbara Supergroup, these felsic units are most likely related to the same plume-dominated processes that formed the basalts that dominate the supergroup. It is very unlikely that modern-style plate tectonic processes played any role in the Paleoarchean evolution of the Pilbara Craton, although some form of non-uniformitarian (e.g. flat) subduction process may have operated.

In stark contrast, the Mesoarchean units of the West Pilbara Terrane and the late-tectonic basins that cover that boundary between the West and East Pilbara Terranes, show clear evidence for modern-style convergent margin processes. Igneous rocks in this belt, which flanks the old eastern cratonic nuclei, have enriched geochemical signatures that cannot be accounted for by crustal contamination. This region is also characterised by a linear magmatic and structural fabric, by the presence of lithologically and geochronologically exotic belts, and by the presence of a broad belt of isotopically more juvenile crust. The collective strength of these arguments provides compelling evidence that a modern-style oceanic arc fringed the East Pilbara Terrane at 3.12 Ga and accreted to that terrane by 2.97 Ga. These assemblages mark the *minimum* age for the birth of modern-style plate subduction process.

Keywords: Mesoarchean; Subduction; Plate tectonics; Pilbara; Pilbara craton; Crustal evolution

1. Introduction

Magmas derived from the subduction of oceanic lithosphere account for the formation of ~80% of Phanerozoic continental crust, but this was not uniformly the case throughout Earth history. The period shortly after planetary accretion, and possibly up to c. 4.4 Ga when the oldest preserved crustal material formed (Wilde et al., 2001), represents the clearest and most extreme case where plate tectonic processes are unlikely to have operated. Heat flow arguments (e.g. Davies, 1993; 1998; Abbott and Hoffman, 1984), and observational evidence from the ancient rock record, indicate that many of the geological processes that operated throughout the Hadean and much of the Archean differ in nature, scale and intensity from those moulding Earth's surface today (e.g. Hamilton, 1998, 2003; McCall, 2003). So—when did plate tectonic, or more particularly, *modern-style* plate tectonic processes[1] begin?

This question should not invite speculation based on a singular criterion. Geochemistry, in particular, has been abused in this way, as recognised, for example, by Ayer et al. (2002). Equally, if we accept that early Earth was not a perfectly uniformitarian system (e.g. Van Kranendonk, 2004), then we

* Corresponding author. Tel.: +61 8 9222 3611; fax: +61 8 9222 3633.
E-mail addresses: hugh.smithies@doir.wa.gov.au (R.H. Smithies), martin.vankranendonk@doir.wa.gov.au (M.J. Van Kranendonk), David.Champion@ga.gov.au (D.C. Champion).

[1] By modern plate tectonic processes, we refer to steep subduction that involves a mantle wedge.

1342-937X/$ - see front matter. Crown Copyright © 2006 Published by Elsevier B.V. on behalf of International Association for Gondwana Research. All rights reserved.
doi:10.1016/j.gr.2006.02.001

must not dismiss proposed evidence for Archean subduction processes (e.g. speculated boninites—Polat et al., 2002; Parman et al., 2001; Shchipansky et al., 2004; Smithies et al., 2004a; Manikyamba et al., 2005) on the basis of an imperfect geological match with Phanerozoic subduction zone assemblages (e.g. Hamilton, 2003).

An array of evidence for pre-Neoproterozoic plate tectonics has been reviewed by Van Kranendonk (2004) and Polat and Kerrich (2006), but the range in estimates for the onset of modern-style subduction and accretion spans from the Paleoarchean (e.g. Burke et al., 1976; Polat et al., 2002; Parman et al., 2001) up to the Neoproterozoic (e.g. Kröner, 1981; Davies, 1992, 1993; Stern, 2005). This lack of consensus on when modern-style plate subduction began is, in part, because such processes almost certainly did not begin everywhere at the same time—there was no magical subduction switch. More likely, subduction began as isolated cases within a crustal regime consisting of thick protocontinental nuclei in oceanic crust, perhaps as far back as the Paleoarchean. Subduction evolved to become a regular process (or, at least, a process with abundantly preserved and readily interpretable evidence), throughout the Neoarchean and Paleoproterozoic (e.g. Van Kranendonk et al., 2004; Polat and Kerrich, 2006), as evidenced by numerous well-established ophiolites (e.g. the 2.0 Ga Purtiniq ophiolite, Scott et al., 1991), and a major process with all the hallmarks of modern subduction in the Neoproterozoic (e.g. Stern, 2005). In the case of the Archean, geological and geochemical evidence for subduction is commonly equivocal because it must be assessed within the context of a geological environment influenced by unusual geochemical components (e.g. TTGs, komatiites) and physical parameters, such as higher mantle temperatures (cf. Nisbet et al., 1993; Davies, 1998) and the interpreted consequences of these (e.g. thicker, more buoyant oceanic lithosphere, smaller plates, more vigorous mantle convection, flat subduction, etc.).

From the geochemical perspective, the best lines of evidence for modern-style subduction are those that point to a mantle source enriched in fluid- and melt-mobile crustal components. At modern convergent margins, fluid and/or melt flux from subducting oceanic lithosphere enriches a variably melt-depleted mantle wedge in large-ion lithophile elements (LILE—e.g. Ba, Sr, Rb, K), light rare earth elements (LREE—La, Ce, Nd), Th and U. This flux also induces partial melting of that metasomatised wedge source, imparting the characteristic LILE and LREE enrichments and HFSE (e.g. Nb, Ta, Zr, Ti) depletions of modern subduction magmas on to the basaltic to andesitic magmas that dominate such tectonic environments. Crustal contamination, however, can produce many of the same geochemical effects and thus geological context is critical to confidently determining an ancient subduction setting.

There are numerous well-documented cases where subduction signatures have been interpreted from Neoarchean igneous rock assemblages (Polat and Kerrich, 2006, and references therein). Importantly, many of these assemblages include independent evidence supporting a convergent margin setting; for example, from structural data, regional lithological architecture or from complex stratigraphic assemblages comprising a diverse range of typically arc-related magmas (e.g. Wyman et al., 2002; Boily and Dion, 2002; Sandeman et al., 2004). However, such clear contextual evidence is commonly lacking for Paleoarchean terranes (e.g. Smithies et al., 2003).

The Pilbara Craton in northwestern Australia contains well-preserved greenstone assemblages that range in age from Paleoarchean to Neoarchean (Van Kranendonk et al., 2002). In this paper, we compare the supracrustal rock assemblages of the Paleoarchean (3.51–3.24 Ga) East Pilbara Terrane with those of the Mesoarchean (c. 3.12 to 2.95 Ga) West Pilbara Terrane and Mallina Basin in the western part of the craton, in terms of geochemical and other geological evidence for modern-style subduction processes. The principle method that we apply to this study is the interpretation of a range of old and new geochemical data, but our interpretations are supported by a range of other lines of geological evidence, including detailed geological mapping and extensive geochronology (see Van Kranendonk et al., 2002). The combined evidence is that modern-style plate tectonic processes played no clear role in the Paleoarchean evolution of the craton (Van Kranendonk et al., 2002; Smithies et al., 2005a,b), but had a fundamental influence during the Mesoarchean (e.g. Smith et al., 1998; Van Kranendonk et al., 2002; Hickman, 2004; Smithies et al., 2005a). The Mesoarchean assemblages mark the *minimum* age for the birth of modern-style plate subduction process in the Pilbara and possibly on Earth.

2. Regional geological setting

The Pilbara Craton contains some of the best-preserved Paleoarchean to Neoarchean stratigraphic succession in the world and can be broadly divided into the lithologically, structurally and geochronologically distinct East, West, and Kurrana Terranes (Fig. 1). The East Pilbara Terrane represents the ancient nucleus of the craton, and has a distinct structural style dominated by ovoid granite complexes mantled by synclinal greenstone belts (Hickman, 1983; Van Kranendonk et al., 2004; Hickman and Van Kranendonk, 2004). The terrane incorporates the well-preserved and well-dated Pilbara Supergroup, comprising four unconformity-bound volcano-sedimentary groups deposited at punctuated intervals from 3.53 to 3.0 Ga (Fig. 2; Van Kranendonk et al., 2002, in preparation). The lowermost Warrawoona Group contains a continuous succession, at least 12 km thick, dominated by pillowed tholeiitic and komatiitic basalt, and locally voluminous komatiite. It also contains locally voluminous felsic volcanic rocks, which cap several (ultra) mafic to felsic volcanic cycles from 3.53 to 3.42 Ga (Hickman and Van Kranendonk, 2004). The unconformably overlying Kelly Group contains up to 8 km of tholeiitic basalt, basaltic komatiite and komatiite, capped by rhyolite, which erupted at between 3.35 and 3.315 Ga. This is, in turn, overlain by the up to 4 km thick, 3.27 to 3.235 Ga komatiitic through to rhyolitic volcanic succession of the Sulphur Springs Group (Buick et al., 2002) and then the dominantly sedimentary Gorge Creek Group. On the northern flank of the East Pilbara Terrane, an upper unit of c. 3.0 Ga (Van Kranendonk et al., 2002) basalt and komatiitic basalt (Cooneeina Basalt) rests conformably on sedimentary rocks of the lower Gorge Creek Group.

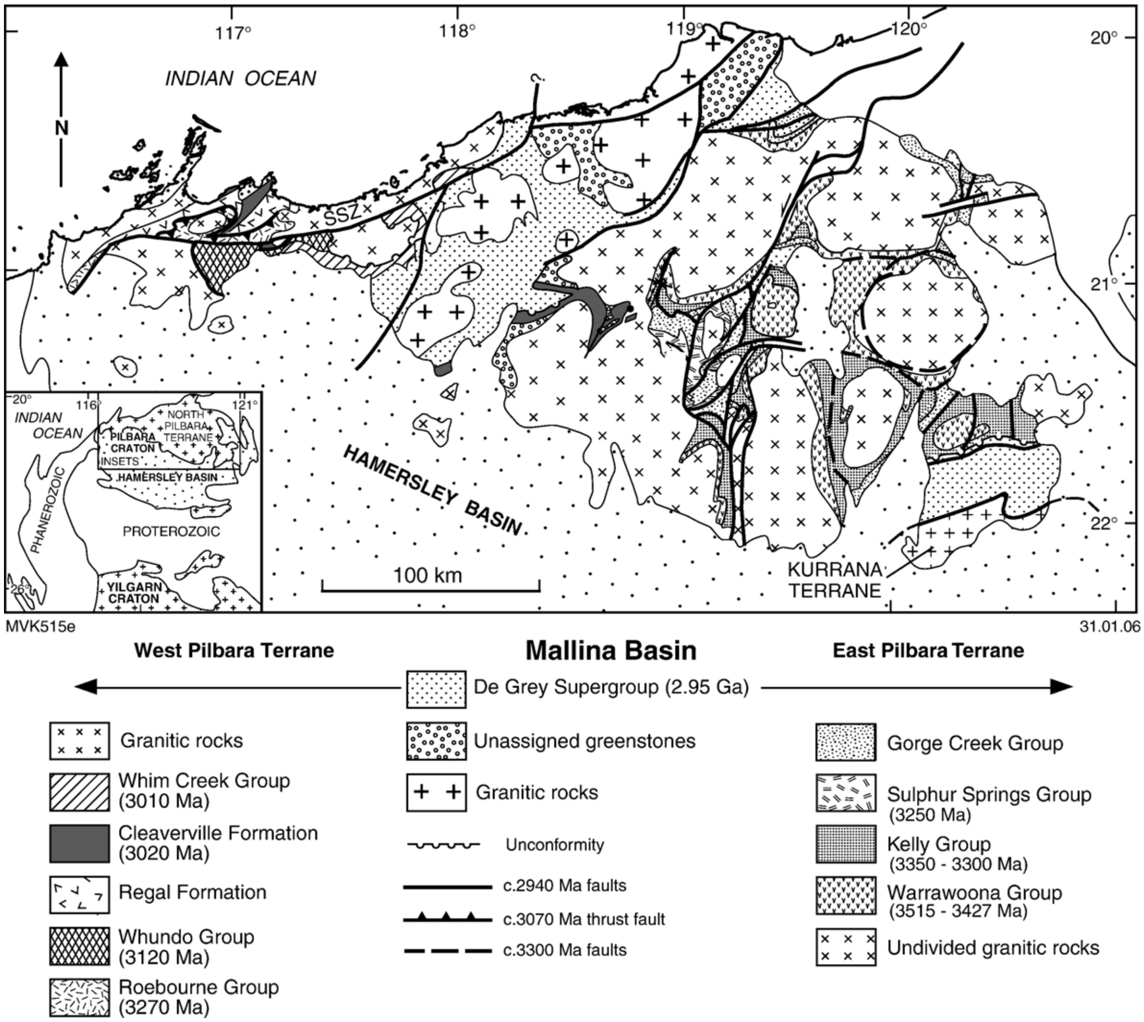

Fig. 1. Regional geology of the Pilbara Craton showing the distribution of the various terranes (SSZ = Sholl Shear Zone).

The West Pilbara terrane (Fig. 1) is composed of a stratigraphic succession that ranges in age from 3.27 to 3.01 Ga, and has a distinct structural style characterised by a prominent northeasterly structural fabric (Hickman, 2004). The main part of this terrane is composed of two distinct lithotectonic assemblages separated by the 1-km-wide Sholl Shear Zone. North of the Sholl Shear Zone is the c. 3.27−3.25 Ga Roebourne Group, an ultramafic–felsic volcanic succession with overlying subordinate clastic metasedimentary rocks.

South of the Sholl Shear Zone is the Whundo Group (Fig. 1), a c. 3.12 to 3.115 Ga sequence of bimodal basaltic to felsic volcanic rocks with a preserved thickness of >10 km thick (Hickman, 1997; Smithies et al., 2005a,b). None of the bounding granite-greenstone terranes have rocks with primary or re-set ages within 100 my of those of the Whundo Group—which represents a geochronologically exotic terrane. The stratigraphic sequence contains no sedimentary material of continental provenance and there is little evidence to suggest that the group was deposited on felsic basement. Nd-isotopic data (Sun and Hickman, 1999) indicate that the group represents juvenile crust. Krapez (1993) interpreted the Whundo Group to represent an arc–forearc allochthon on the basis of a bimodal volcanic stratigraphy, whereas Smith et al. (1998) and Krapez and Eisenlohr (1998) favoured a back-arc setting. Hickman (2004) suggested the Whundo Group was deposited on oceanic-type crust in a post-3240 Ma rift between the east Pilbara and the Roebourne Group.

Overlying the Whundo Group is the dominantly felsic volcano–sedimentary sequence of the 3.01 Ga Whim Creek Basin, which according to Pike and Cas (2002) is a continental arc, developed during outboard accretion of the Whundo and Roebourne terranes (Van Kranendonk et al., in preparation).

Overlying the older (>3.0 Ga) rocks of the Pilbara Craton is the dominantly sedimentary De Grey Supergroup, deposited between c. 2.97 and 2.93 Ga (Fig. 1). The main depositional basin for this supergroup was the ENE-trending Mallina Basin, which, along with the more localised Goldsworthy Basin to the east, developed along the western and northern margins of the East Pilbara Terrane, and covers the contact between the East and West Pilbara Terranes. The main period of deposition within the Mallina Basin occurred between 2.97 Ga and 2.955 Ga with medium to coarse-grained wacke and conglomerate overlain by medium- to fine-grained

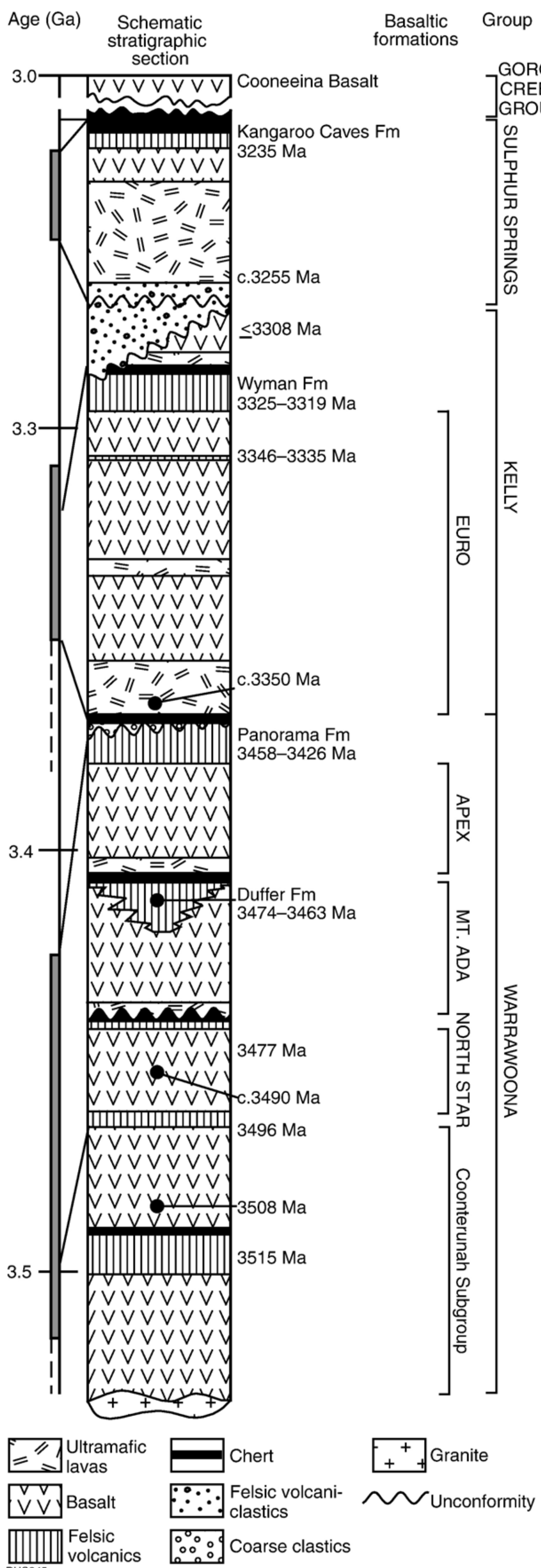

Fig. 2. Schematic stratigraphic section through the Paleoarchean Pilbara Supergroup of the East Pilbara Terrane, showing relative thickness of respective units. Geochronological details are from Van Kranendonk et al. (2002).

siliciclastic turbidites (Smithies et al., 2001). Along the northwestern margin of the basin, volcaniclastic turbidites (Bookingarra Group) filled local fault-bounded depocentres sourced primarily from the unconformably underlying c. 3.01 Ga Whim Creek Group (Pike, 2001; Pike and Cas, 2002), which forms the youngest component of the West Pilbara Terrane. Subaqueous flows of siliceous high-Mg basalt (Louden Volcanics, Mount Negri Volcanics) dominate the upper part of the Bookingarra Group and form a widespread discontinuous layer within siliciclastic turbidite units in the southern and central parts of the Mallina Basin. Their sub-volcanic gabbroic equivalents are widespread throughout the

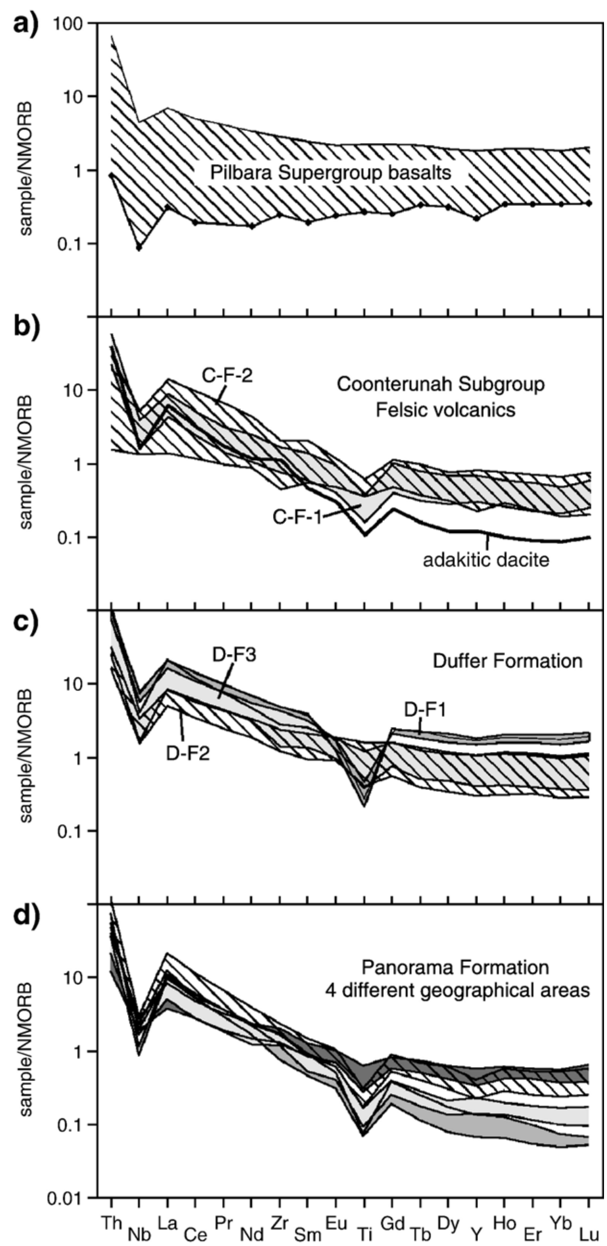

Fig. 3. MORB normalised trace element diagrams for supracrustal units of the Pilbara Supergroup. (A) Shows the field for ~130 basalts (MgO < 12 wt.%) from the Warrawoona Group. (B, C and D) Show the various trace element enriched basalt–dacite units. (Normalising values from Sun and McDonough, 1989.)

southern and eastern part of the basin and occur up to 50 km northwest of the basin, where they intrude the West Pilbara Terrane. Rocks with compositions similar to boninites or to cratonic norites also form a ~300-m-thick sub-volcanic sill (Smithies, 2002) in the southern part of the basin. The available geochronology (Smithies et al., 2004b; Van Kranendonk et al., 2002 and references therein) indicates that this mafic magmatism (informally the Mallina mafic suite) occurred less than 20 my before the intrusion of an extensive high-Mg diorite (sanukitoid) suite emplaced between 2.955 and 2.945 Ga (Smithies and Champion, 2000). Basalts that are contemporaneous, and compositionally similar to, the Mallina mafic suite also occur in the Goldsworthy Basin.

While the lower Bookingarra Group contains a minor felsic volcanic component (e.g. Pike, 2001; Pike and Cas, 2002), the main fill of the Mallina Basin contains no evidence of the felsic volcanic detritus that might be expected in a basin fringing a contemporaneous arc. Provenance studies of dated detrital zircon populations show that sources on both sides of the Mallina Basin made significant contributions to the sediment fill (Smithies et al., 2001). The tectonic setting of the Mallina Basin remains unclear, however, there is no regional evidence for subduction contemporaneous with formation of the Mallina Basin and associated Mallina mafic suite and the sanukitoid suite.

3. Geochemical data set

Our geochemical data set consists of ~400 geochemical analyses of mafic to felsic volcanic rocks sampled from throughout the Pilbara Craton from units covering the age range between c. 3.51 and 2.94 Ga. These samples were collected throughout the ~10-year span of a detailed mapping program by the Geological Survey of Western Australia and Geoscience Australia, which was aimed at vastly increasing our understanding of the geological evolution of the Pilbara Craton. Care was taken to ensure samples were fresh, without visible veins or alteration. Nevertheless, all samples have been recrystallised at greenschist facies, as is typical of Archean supracrustal rocks. The age and stratigraphic associations of the sampled rocks are very well constrained within a significantly revised stratigraphic framework set out by Van Kranendonk et al. (in preparation).

All analyses were undertaken at Geoscience Australia. Analytical details, and most analyses, can be obtained in Smithies and Champion (2000) and Smithies et al. (2004a, 2005a,b). New data for the felsic rocks of the Pilbara Supergroup can be obtained from the author upon request.

4. The East Pilbara Terrane—a non-uniformitarian paradigm for the formation of the ancient cratonic nucleus

Ideas on the formation of crust in the East Pilbara Terrane has been controversial. Several detail structural studies have interpreted a horizontal component of deformation in the structural evolution of the East Pilbara Terrane and compared it favourably with Alpine-style orogenesis in a plate-tectonic regime (cf. Bickle et al., 1985; Barley, 1997; Kloppenburg et al., 2001; Zegers et al., 2001; Blewett, 2002). It should be noted, however, that the Pilbara Supergroup is not a collection of structurally bound allochthonous, or laterally accreted, packages more typical of modern accreted margins and of Neoarchean terranes interpreted to be subduction related (e.g. Tomlinson et al., 2003). Rather, detailed mapping, structural and metamorphic interpretations, and extensive geochemistry and geochronology have shown that the supergroup comprises a cumulative, 20 km thick, sequence of autochthonous and consistently upward-younging, volcanic rocks and subordinate sedimentary rocks deposited in four groups (Hickman, 1983; Van Kranendonk et al., 2002, in preparation; Hickman and Van Kranendonk, 2004). The lowest Warrawoona Group, deposited between 3.52 and 3.42 Ga, consists of a continuous succession of eight ultramafic to felsic volcanic cycles that more closely resembles thick oceanic plateau crust (e.g. Arndt et al., 2001; Van Kranendonk et al., 2002) and it has been suggested that crustal evolution was primarily a result of a series of mantle plume events (Van Kranendonk and Pirajno, 2004; Smithies et al., 2005a).

Geochemical analyses of approximately 250 volcanic rocks, spanning most of the stratigraphy of the Pilbara Supergroup (c. 3.51 to 3.2 Ga), show a sequence that is greatly dominated, at every stratigraphic level, by basalts (Fig. 2). The least fractionated of these have trace-element patterns reflecting a mantle source region that ranged in composition from close to that of primitive mantle (Condie, 2005) to compositions as depleted as MORB source (Fig. 3) (e.g. Zr/Nb range from 11 to 30 c.f. values of 16 and 32 for primitive mantle and NMORB, respectively—Sun and McDonough, 1989). The lower part of the supergroup does include three units where a basalt–dacite cycle includes a significant proportion of basaltic and andesitic material (Fig. 2), some with trace element enrichment patterns (Table 1) resembling those of modern continental arcs.

Enriched basalt–dacite series occur within the c. 3.51 Ga Coonterunah Subgroup, at the preserved base of the Pilbara Supergroup, including the C-F1 andesite to dacite series (55 to 65 wt.% SiO_2) and the overlying basalt to andesite C-F2 series (47.5 to 57.5 wt.% SiO_2). A single dacite (69 wt.% SiO_2) has a composition typical of Archean TTG, including low Yb (0.98 ppm) and very high La/Yb (26.7), reflecting a source with residual garnet. Basaltic rocks within the C-F2 series show considerable overlap in major and trace element compositions with the tholeiites of the lower Coonterunah Subgroup (Table 1).

The 3.47 Ga Duffer Formation comprises three compositionally distinct enriched series. D-F1 rhyolites (68.8–75 wt.% SiO_2) are very rare but occur throughout the pile. They have high Fe, HREE, Zr and Nb (Table 1), and share these features with felsic volcanic rocks that have elsewhere been interpreted as strongly fractionated tholeiites (e.g. Hollings and Kerrich, 2000), although moderately high K_2O (~2.6 wt.%) and notable Nb and Ti anomalies likely also require a degree of crustal assimilation (e.g. Smithies et al., 2005a). The main

Table 1
Median compositions and standard deviation for rocks of the East Pilbara Terrane

	Warrawoona Group basalt		Coonterunah Subgroup basalt		Coonterunah Subgroup C-F1		Coonterunah Subgroup C-F2		Coonterunah Subgroup adakite	Duffer Fm. D-F1		Duffer Fm. D-F2	
	(n=60)		(n=17)		(n=19)		(n=15)		(n=1)	(n=3)		(n=14)	
	Median	S.D.	Median	S.D.	Median	S.D.	Median	S.D.		Median	S.D.	Median	S.D.
SiO_2	48.79	2.62	49.04	2.19	58.61	3.53	53.44	5.17	66.06	70.77	4.33	56.08	4.85
SiO_2(a)	51.00	1.81	50.25	1.59	59.72	3.43	54.14	3.90	66.06	72.57	3.11	59.44	4.56
TiO_2	1.05	0.39	1.11	0.29	0.88	0.20	1.42	0.32	0.48	0.31	0.15	0.73	0.35
Al_2O_3	13.17	1.52	14.25	1.50	15.70	1.06	15.08	1.91	15.04	12.90	0.40	15.87	1.02
$Fe_2O_3^T$	13.13	1.94	14.49	1.68	8.17	2.08	13.44	2.75	3.58	3.73	0.95	7.43	3.12
MnO	0.20	0.05	0.26	0.07	0.13	0.05	0.24	0.09	0.05	0.06	0.03	0.11	0.05
MgO	6.17	2.27	6.32	3.45	2.74	0.86	3.85	1.25	1.14	0.53	0.56	3.16	1.81
CaO	9.69	2.46	10.41	3.30	6.65	1.45	6.25	2.27	3.28	2.12	1.67	6.06	1.47
Na_2O	2.28	1.06	2.31	0.86	3.69	0.66	3.10	1.39	5.06	4.61	1.69	4.05	1.29
K_2O	0.16	0.29	0.26	0.23	0.73	0.33	0.56	0.41	0.90	2.60	0.29	0.84	0.77
P_2O_5	0.10	0.05	0.10	0.04	0.20	0.06	0.33	0.13	0.12	0.05	0.04	0.14	0.05
$Mg^\#$	48	9	45	11	42	8	36	7	39	24	9	44	10
ppm													
Cr	187	346	189	517	87	95	38	65	12	9	4.0	35	106
Ni	82	96	92	160	55	28	45	45	18	10	1.5	46	33
Sc	41	6	46	5	19	3.3	20	6	7	7	1.5	12	7
Rb	2.2	8.7	3.6	9.2	24.5	10.0	11.5	13.5	17.3	61.7	29.6	22.6	22.9
Cs	0.23	0.73	0.12	0.70	1.02	0.49	0.45	0.58	0.5	1.38	2.04	1.06	0.63
Ba	43	645	48	1152	185	97	76	176	334	802	196	293	158
Sr	100	54	99	28.6	170	40.1	157	60	174	151	101	433	297
Nb	3.8	1.6	3.7	1.1	10.	2.0	11.2	4.9	7.9	14.9	2.2	4.7	1.1
Zr	78	33	75	25	201	36	198	82	190	315	20	102	22
Y	23.0	8.1	21.6	6.7	32	5.8	33	10.3	11.5	42	3.4	16.2	5.4
Th	0.6	0.3	0.5	0.2	4.8	1.0	2.7	1.9	5.7	9.6	1.4	2.6	0.5
La	5.3	2.1	4.1	1.5	24.4	4.6	19.5	11.3	26.2	45.6	6.0	15.0	2.3
Ce	13.8	5.1	11.6	3.4	45	8.9	42.7	23.0	44.5	91.6	12.1	29.5	4.9
Pr	2.1	0.74	1.8	0.54	5.4	1.1	5.9	2.9	4.8	11.1	1.3	3.8	0.68
Nd	10.3	3.5	8.9	2.6	23.0	4.6	25.2	10.6	19.2	43.7	5.3	15.4	3.0
Sm	2.91	0.98	2.52	0.77	5.23	0.96	6.26	1.89	3.28	8.65	0.83	3.42	0.78
Eu	1.04	0.34	0.97	0.25	1.35	0.26	1.88	0.43	0.90	1.49	0.23	1.08	0.24
Gd	3.65	1.19	3.20	0.93	5.36	0.99	6.10	1.59	2.68	8.04	0.67	3.20	0.90
Tb	0.65	0.21	0.63	0.16	0.83	0.15	0.97	0.26	0.35	1.33	0.16	0.51	0.16
Dy	4.03	1.30	3.80	1.07	5.18	0.91	5.86	1.51	1.89	7.55	0.93	3.00	0.96
Ho	0.92	0.29	0.86	0.24	1.09	0.18	1.27	0.34	0.36	1.69	0.21	0.64	0.23
Er	2.57	0.83	2.45	0.68	2.98	0.50	3.58	0.97	0.98	4.82	0.58	1.88	0.63
Yb	2.49	0.80	2.47	0.64	2.85	0.45	3.14	1.00	0.98	4.79	0.72	1.77	0.60
Lu	0.41	0.14	0.41	0.12	0.49	0.08	0.50	0.17	0.16	0.77	0.11	0.28	0.10
La/Nb	1.3	0.2	1.2	0.2	2.4	0.2	1.5	0.5	3.3	3.1	0.1	3.1	0.6
La/Yb	2.0	0.5	1.8	0.5	8.9	1.2	6.0	1.8	7.8	8.9	0.7	8.4	2.6
La/Sm	1.67	0.30	1.54	0.29	4.61	0.47	3.07	1.09	7.99	5.06	0.30	4.37	0.48
Gd/Yb	1.48	0.15	1.45	0.13	1.93	0.16	1.80	0.27	2.73	1.68	0.13	1.84	0.27
Th/Nb	0.16	0.04	0.13	0.03	0.47	0.09	0.18	0.17	0.73	0.65	0.01	0.50	0.11
K_2O/Na_2O	0.06	0.52	0.11	0.15	0.20	0.09	0.14	6.63	0.18	0.56	0.64	0.23	0.30

Basalts from the Warrawoona Group include only those rocks with MgO < 12 wt.% and basalts from the Coonterunah Subgroup form a subset of these data. Panorama Formations 1, 2, 3 and 4 represent four geographically separated units from this formation. SiO_2(a) = silica value calculated volatile free. $Fe_2O_3^T$ = all Fe calculated as Fe_2O_3. Data for the Kangaroo Caves Fm. are from Brauhart (1999).

pile comprises the D-F2 and overlying D-F3 basalt to dacite series, which overlap extensively in silica range (D-F2 = 51.8–65 wt.% SiO_2; D-F3 = 52.4–68.8 wt.% SiO_2). Rocks of the 3.43 Ga Panorama Formation show the widest compositional range and unsilicified samples typically have between 54 and 76.9 wt.% SiO_2, and average ~67.5 wt.%. They form discrete geographical centres of compositionally distinct volcanics.

4.1. Origin of the trace-element enriched rocks

The enriched series of the Coonterunah Subgroup (CF-1 and CF-2) show features more typical of fractionating tholeiitic series than of the calk-alkaline series or of the Archean TTG series. They have low K_2O (< 1.0 wt.%) and are Fe-rich; the C-F2 series, in particular, has similarly low La/Nb and Th/Nb ratios as the lower Coonterunah basalts and show no significant

Duffer Fm. D-F3		Panorama Fm. 1		Panorama Fm. 2		Panorama Fm. 3		Panorama Fm. 4		Kangaroo Caves Fm.—rhyolite		Cooneenia Basalt	
($n=10$)		($n=10$)		($n=3$)		($n=6$)		($n=4$)		($n=11$)		($n=10$)	
Median	S.D.	Median	S.D.	Median	S.D.	Median	S.D.	Median	S.D.	Median	S.D.	Median	S.D.
59.02	5.38	66.83	5.81	82.65	4.62	57.75	6.17	74.78	2.52	75.41	1.39	52.29	1.39
61.30	4.99	67.86	5.51	86.22	4.15	61.08	5.92	77.07	3.09	76.33	1.36	54.48	1.01
0.72	0.26	0.48	0.07	0.15	0.00	0.77	0.24	0.23	0.06	0.24	0.09	0.52	0.06
15.43	0.74	15.74	1.64	11.56	1.09	15.42	1.27	13.08	2.34	11.85	0.60	14.27	0.24
6.99	2.51	3.27	1.57	0.14	0.20	6.51	2.15	0.74	0.90	2.53	0.81	10.10	0.66
0.14	0.04	0.08	0.05	0.01	0.02	0.10	0.04	0.01	0.01	0.05	0.01	0.17	0.02
3.19	1.64	1.50	1.15	0.02	0.58	2.86	1.21	0.81	0.81	0.33	0.15	6.77	0.50
4.45	1.72	4.96	2.40	0.02	1.04	5.54	0.85	0.09	0.04	1.16	0.34	9.88	0.73
4.66	1.42	3.58	1.65	0.02	0.02	4.91	1.29	0.05	0.09	2.97	0.24	1.77	0.52
1.34	0.70	1.94	2.07	0.24	2.77	0.73	0.57	6.95	1.22	4.40	0.28	0.78	0.25
0.17	0.03	0.12	0.04	0.03	0.01	0.17	0.04	0.06	0.02	0.05	0.02	0.06	0.01
49	7	48	6	21	34	49	3	63	13	22.74	7.28	57	3
65	69	49	21	16	11	106	68	14	9			235	49
51	54	24	12	11	1	55	28	17	3			97	11
14	5	9	2	3	1	18	7	4	1			37	5
25	18	71	31	4	38	34	17	121	15			27	10
0.97	0.79	2.63	1.33	0.14	0.50	0.98	0.95	1.55	2.75			0.48	0.10
618	509	337	318	58	1384	164	117	323	66			202	58
427	168	149	47	40	5	176	56	27	2.6	71	16	152	34
5.9	1.4	6.8	0.8	3.1	0.4	6.4	0.8	5.5	0.7	13.0	1.5	2.3	1.0
136	24	184	15	110	22	155	22	133	20	203	52	57	17
15.6	4.6	12.1	2.3	4.7	1.4	16.0	3.3	6.6	1.6	50.0	11.3	16.1	1.8
6.4	2.3	6.6	2.2	7.5	2.1	4.2	1.2	3.2	1.7	26.1	8.9	1.7	0.6
28.7	5.8	32.1	8.6	30.1	1.9	19.8	4.0	17.3	9.0	46.8	6.9	7.4	2.8
53.3	8.7	60.4	13.6	49.2	3.0	39.2	6.2	31.5	9.3	92.3	12.2	15.2	5.2
6.6	0.9	6.6	1.4	5.3	0.5	4.6	0.7	3.7	1.2			1.7	0.6
25.5	3.1	24.1	4.5	17.9	2.3	17.6	2.6	14.0	4.1			6.9	2.5
4.7	0.7	4.3	0.6	2.6	0.7	3.5	0.5	2.5	0.5	6.9	1.2	1.7	0.6
1.25	0.20	1.17	0.17	0.66	0.14	1.02	0.16	0.70	0.11	1.05	0.54	0.61	0.10
3.54	0.75	3.14	0.51	1.63	0.47	3.33	0.43	1.82	0.31			2.18	0.43
0.48	0.12	0.45	0.08	0.21	0.07	0.57	0.08	0.27	0.05	1.20	0.29	0.41	0.06
2.82	0.76	2.51	0.51	0.91	0.31	3.39	0.53	1.33	0.21			2.71	0.31
0.58	0.18	0.51	0.11	0.16	0.05	0.76	0.10	0.26	0.04			0.63	0.06
1.67	0.54	1.34	0.32	0.39	0.10	2.09	0.26	0.69	0.11	5.29	1.17	1.87	0.16
1.53	0.50	1.14	0.37	0.32	0.06	1.94	0.29	0.63	0.13			1.89	0.13
0.24	0.09	0.19	0.06	0.05	0.01	0.33	0.06	0.10	0.02	0.78	0.17	0.31	0.02
5.1	1.2	5.0	1.0	9.9	0.77	2.9	0.56	2.9	1.6	3.6	0.7	2.8	0.5
18.3	9.5	27.6	9.1	93.9	12.8	10.4	2.8	28.1	13.6	7.8		4.0	1.4
6.35	1.48	8.27	1.33	11.52	3.24	5.26	1.03	7.44	2.01	6.42	1.24	3.88	0.62
2.38	0.30	2.46	0.34	5.09	0.59	1.77	0.14	2.78	0.31			1.18	0.18
1.13	0.33	0.98	0.26	2.40	0.45	0.62	0.17	0.54	0.30	1.86	0.76	0.70	0.06
0.34	0.30	0.53	20	13.4	143	0.15	0.23			1.51	0.16	0.42	0.22

(continued on next page)

increase in these ratios through significant increases in La and Th concentrations (Fig. 4; Table 1). HREE and Y concentrations are positively correlated with SiO_2 content and La/Yb ratios, a feature of fractionating tholeiitic series that contrasts with trends in Archean TTG series (Fig. 5). Slightly higher La/Nb and La/Yb in the C-F1 series likely reflect some form of interaction between mafic magmas (or their source) and crustal material. Ratios of similarly highly incompatible trace elements (e.g. La/Th, Th/Nb, La/Zr) in the C-F1 rocks match those of the single sample of TTG-like dacite, and low Yb and high La/Yb in the C-F1 rocks (Table 1) are consistent with small amounts of contamination of basaltic magmas with this TTG-like material. Very modest changes in La/Nb and Th/Nb ratios over significant La and Th ranges suggest that such contamination likely occurred before closed system fractionation that did not involve hornblende—presumably in a deep crustal chamber.

Table 1 (*continued*)

	Whundo Gp. tholeiitic basalt		Whundo Gp. boninite		Whundo Gp. calc-alkaline		Whundo Gp. adakitic dacite		Whundo Gp. Nb-rich basalt	
	($n=14$)		($n=6$)		($n=20$)		($n=4$)		($n=2$)	
	Median	S.D.	Median	S.D.	Median	S.D.	Median	S.D.	Median	S.D.
SiO_2	48.22	1.97	50.35	1.98	53.89	3.09	59.73	4.52	50.25	2.05
SiO_2(a)	50.77	1.23	52.63	1.47	55.94	2.64	63.01	3.21	52.37	1.54
TiO_2	1.44	0.17	0.31	0.07	0.82	0.28	0.71	0.27	1.67	0.47
Al_2O_3	13.56	0.55	16.60	0.35	15.82	1.02	14.57	0.57	15.34	0.91
$Fe_2O_3^T$	13.86	0.79	10.39	0.35	8.97	1.64	6.28	1.00	12.18	2.32
MnO	0.20	0.01	0.20	0.02	0.15	0.03	0.13	0.04	0.17	0.01
MgO	5.99	0.48	8.96	0.68	5.16	1.24	3.00	0.91	5.38	0.07
CaO	9.70	1.11	7.43	0.78	7.54	1.37	5.22	1.91	6.15	2.70
Na_2O	2.17	0.51	1.44	0.36	2.55	0.89	3.86	1.44	2.14	0.21
K_2O	0.14	0.20	0.55	0.51	0.88	0.76	0.75	0.67	2.26	1.12
P_2O_5	0.15	0.02	0.06	0.01	0.17	0.05	0.16	0.05	0.40	0.08
$Mg^{\#}$	46	3	63	2	53	5	51	8	47	4
ppm										
Cr	120	21	176	55	124	59	58	63	105	54
Ni	79	9	80	11	64	33	51	37	41	23
Sc	39	4	45	4	30	8	17	3	31	5
Rb	0.95	6.1	20	22	25	21	26	26	42	8.8
Cs	0.18	0.19	3.04	3.19	1.12	0.82	0.90	0.30	1.30	0.21
Ba	101	147	77	51	190	179	182	121	754	261
Sr	142	59	87	14.5	153	85	154	81	251	137
Nb	4.7	0.6	1.2	0.9	4.9	1.5	6.3	1.2	9.6	1.3
Zr	106	15	20	19	114	36	157	25	153	13
Y	39	5.4	7.7	3.9	22	7.	19	3.5	33	6
Th	0.7	0.1	0.4	0.3	1.8	0.9	3.7	0.6	1.3	0.3
La	5.9	0.82	2.7	1.7	11	3.5	18	2.7	15	0.93
Ce	16.1	2.0	6.2	4.4	26	7.4	41	5.5	40	4.2
Pr	2.5	0.29	0.80	0.55	3.4	0.91	4.9	0.60	5.5	0.79
Nd	12.26	1.44	3.49	2.23	14.31	3.56	18.64	1.97	24.23	4.44
Sm	4.0	0.45	0.93	0.53	3.5	0.88	3.9	0.43	5.8	1.2
Eu	1.34	0.18	0.31	0.11	0.99	0.21	1.02	0.15	1.79	0.38
Gd	5.17	0.63	0.98	0.54	3.40	0.92	3.49	0.50	5.84	1.30
Tb	0.97	0.13	0.17	0.10	0.56	0.14	0.56	0.10	0.95	0.20
Dy	5.96	0.78	1.15	0.59	3.30	1.09	3.17	0.58	5.25	1.03
Ho	1.30	0.18	0.26	0.13	0.73	0.23	0.68	0.14	1.07	0.21
Er	3.88	0.54	0.84	0.38	2.19	0.69	1.97	0.39	3.17	0.56
Yb	3.74	0.54	1.00	0.39	2.21	0.69	1.86	0.40	3.00	0.57
Lu	0.55	0.08	0.18	0.05	0.34	0.12	0.28	0.05	0.43	0.06
La/Nb	1.2	0.07	2.2	1.1	2.2	0.35	3.1	0.45	1.6	0.12
La/Yb	1.6	0.24	2.7	0.64	5.1	1.3	9.3	2.5	5.0	0.63
La/Sm	1.45	0.12	2.85	0.56	3.25	0.57	4.68	0.54	2.60	0.40
Gd/Yb	1.39	0.07	1.00	0.15	1.56	0.19	1.91	0.27	1.94	0.07
Th/Nb	0.14	0.02	0.36	0.15	0.35	0.11	0.67	0.14	0.14	0.05
K_2O/Na_2O	0.06	0.09	0.29	0.37	0.32	1.73	0.19	0.38	1.09	0.63

The enriched series of the Duffer and Panorama Formations, in contrast, show some features more typical of modern calk-alkaline series or the Archean TTG series. They show strong overlap with (for example) the compositional range for calk-alkaline rocks related to the continental Andean arc system, including similarly high ranges in La/Nb, Th/Nb and La/Yb (Fig. 5). They contrast with Andean arc rocks, however, in having a lower proportion of rocks in the basaltic silica range and in having typically more sodic compositions ($K_2O/Na_2O<0.6$), and in these respects are more like the Archean TTG series (Fig. 5).

Viewing the compositions of the enriched volcanic series of the lower Pilbara Supergroup through time, several broad secular trends become apparent. With decreasing age, the rocks become generally more silicic and Al-rich (at a given SiO_2) and range to generally higher La/Sm, La/Yb and La/Nb

Whundo Gp. rhyolite		Mallina Basin basalt		Mallina Basin boninite-like rock		Goldsworthy Basin basalt		High-Mg Diorite suite	
(n=9)		(n=35)		(n=6)		(n=3)		(n=20)	
Median	S.D.	Median	S.D.	Median	S.D.	Median	S.D.	Median	S.D.
75.12	2.69	55.54	1.92	52.67	4.46	54.76	0.82	65.16	2.54
76.76	2.50	56.26	1.70	54.22	>3.91	55.86	1.57	66.43	2.60
0.25	0.11	0.62	0.23	0.25	0.05	1.02	0.20	0.44	0.08
11.11	0.69	14.37	1.47	16.89	2.45	14.28	0.44	14.62	0.62
3.71	0.96	9.36	1.25	9.22	1.06	10.72	1.83	4.84	1.29
0.05	0.01	0.15	0.02	0.17	0.03	0.16	0.02	0.06	0.02
0.93	0.66	5.53	1.43	8.43	6.14	5.40	0.11	2.31	0.92
1.83	1.16	7.96	1.90	7.72	1.13	6.92	1.15	3.71	0.86
2.96	1.12	2.60	0.88	1.69	0.89	3.24	0.60	4.09	0.36
1.35	0.88	0.89	0.58	0.28	0.40	1.56	0.47	2.21	0.53
0.04	0.02	0.10	0.02	0.04	0.01	0.14	0.00	0.22	0.07
32	10	55	7	66	8	50	5	48	5
9	19	134	211	417	1169	149	96	92	56
10	7	95	36	100	114	71	51	41	25
8	4	26	5	39	5	26	6	9	3
26	26	33.4	24.7	9.5	19.9	39.1	17.5	98	16.9
0.82	0.69	0.90	3.06	3.03	10.53	0.38	0.19	7.65	4.32
300	167	461	416	63	63	506	80	857	239
92	39	219	98	139	59	256	17.9	485	63
19.6	3.5	6.1	2.4	1.2	0.52	5.8	0.38	6.7	1.7
361	63	122	51	34	10.1	110	9.6	153	21
73	22	18.4	7.8	11.6	1.8	22.3	1.4	13.6	3.1
7.1	0.7	5.0	1.8	0.79	0.18	3.3	0.21	11.0	3.2
37	4.4	19.4	7.1	5.6	1.4	15.2	0.91	47.4	11.9
87	14	37.7	14.7	11.1	3.0	33.2	1.4	90	24.3
11.5	1.8	4.5	1.8	1.3	0.35	3.6	0.06		
46.59	8.19	17.4	6.7	4.9	1.23	16.1	0.20	35.3	8.7
11.2	2.4	3.7	1.4	0.97	0.24	3.7	0.24	5.7	1.3
1.92	0.62	1.00	0.25	0.30	0.08	1.16	0.06	1.40	0.32
10.65	2.91	3.80	1.21	1.06	0.22	4.13	0.32	4.15	0.91
1.82	0.56	0.57	0.20	0.21	0.03	0.70	0.05	0.40	0.13
10.96	3.30	3.22	1.18	1.45	0.26	3.79	0.25	2.50	0.55
2.44	0.73	0.65	0.26	0.38	0.07	0.77	0.05	0.40	0.10
7.49	2.26	1.73	0.72	1.21	0.51	2.25	0.16	1.20	0.30
7.63	2.25	1.72	0.79	1.53	0.23	2.11	0.17	1.00	0.25
1.22	0.36	0.26	0.13	0.27	0.05	0.30	0.02	0.10	0.07
1.9	0.19	3.2	0.30	4.7	3.6	2.6	0.33	7.0	1.0
4.4	0.64	8.2	2.5	3.5	0.57	7.1	1.1	7.8	0.00
3.34	0.32	5.24	0.27	5.59	0.23	3.88	0.46	8.17	1.04
1.32	0.07	1.60	0.39	0.66	0.06	2.03	0.04	3.61	0.58
0.35	0.07	0.86	0.24	0.66	0.60	0.56	0.08	1.67	0.20
0.33	0.38	0.36	0.26	0.22	0.69	0.48	0.27	0.56	0.15

ratios (Fig. 6). These trends are consistent with gradual thickening of the lower Pilbara Supergroup pile. They could be interpreted in terms of either a general increase in the pressure of magma genesis and the control of residual garnet on magma compositions, or an increasing contribution of a source (or contaminant) component that was formed at high-pressure, such as Archean TTG. The geochemical features are most compatible with a progressively greater degree of interaction between basalt and TTG, either via greater contamination of basaltic melt by TTG or melting of a basaltic crust with a successively higher component of interleaved TTG material. It is interesting to note that the upper felsic volcanic units of the Pilbara Supergroup (e.g. some units in the 3.43 Ga Panorama Formation, as well as the 3.32 Ga Wyman Formation of the Kelly Group, and 3.24 Ga Kangaroo Caves Formation of the Sulphur Springs Group—Table 1) along with their sub-volcanic

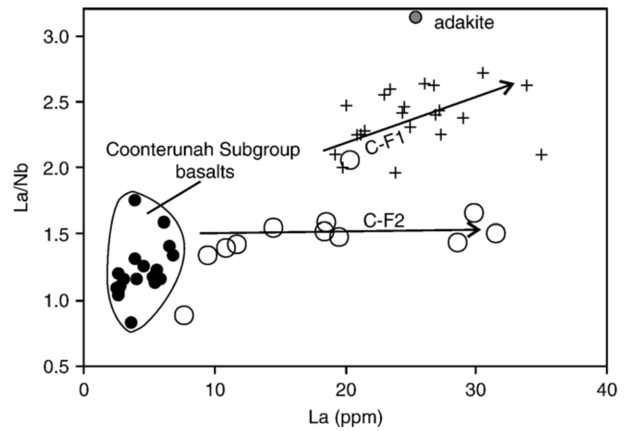

Fig. 4. Variation diagram showing La/Nb vs. La (ppm) for basalts (filled circles) and the trace element enriched basalt–dacite units.

equivalents, are strongly potassic crustal melts (Jahn et al., 1981; Glikson et al., 1987; Collins, 1993; Cullers et al., 1993; Brauhart, 1999; Champion and Smithies, 2001). Thus, felsic volcanic units progressively evolve from tholeiitic to TTG-like to intra-crustal high-K melts—a trend which mirrors that seen in the granites of the region and can be explained in terms of progressive recycling of an initially basaltic crust (Champion and Smithies, 2001). It is important to note that, in the case of the East Pilbara Terrane, this compositional evolution occurs on a time span of ~300 my and occurs within a geographically restricted area, with no temporal polarity.

5. The west Pilbara Craton and Mallina Basin—clear signs of modern-style subduction

The West Pilbara Terrane and the basins that host the De Grey Supergroup flank the western and northern margin of the ancient East Pilbara Terrane (Fig. 1). The West Pilbara Terrane essentially comprises a series of elongate east–northeast trending belts, with independent stratigraphy and structural histories. One major structural boundary, the east–northeast-trending Sholl Shear Zone (SSZ—Fig. 1), has a major sinistral displacement at 3.05–3.02 Ga and a further 40 km dextral displacement at c. 2.92 Ga (Hickman, 2004) and provides unequivocal evidence for major plate tectonic processes. The northern part of the terrane includes granites as old as 3.27 Ga and volcanic rocks in this region preserve isotopic evidence for basement with components as old as the older components of the East Pilbara Terrane. The Whundo belt, in the southern part of the West Pilbara Terrane is a geochronologically exotic terrane dominated by c. 3.12 Ga submarine volcanic rocks of the Whundo Group, with juvenile isotopic compositions and with little physical, chemical or isotopic evidence for an older felsic basement.

The late basins that host the 2.97–2.93 Ga De Grey Supergroup can essentially be regarded as an elongate series of fluvial sediment and turbidite filled basins. Some of these basins include LREE-enriched basaltic rocks. The known geographical extent of this magmatism is ~350 km, in an east–northeasterly direction flanking the East Pilbara–West Pilbara terrane boundary (Fig. 7). This zone roughly corresponds to an isotopic domain, primarily within the late basins, marked by syn- to late-basin formation mafic to felsic magmas with Nd depleted-mantle model ages close to the magmatic age of the Whundo Group (Fig. 7).

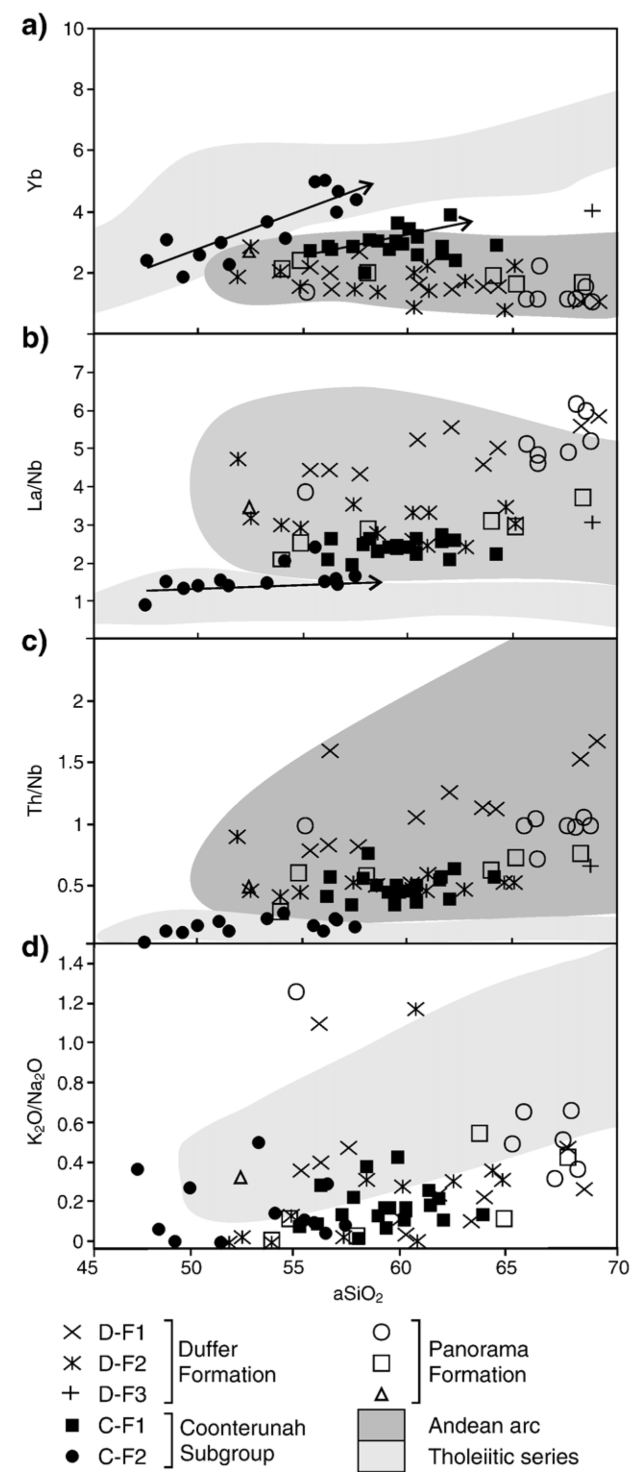

Fig. 5. Variation diagrams showing Yb (ppm), La/Nb, Th/Nb, and K_2O/Na_2O vs. SiO_2 (anhydrous) [aSiO_2] for trace element enriched basalt–dacite units of the Warrawoona Group (Pilbara Supergroup). Shaded field are for a range of subduction related rocks from the Andean arc and for tholeiitic basalts to rhyolites from Iceland (data from the GEOROC database—http://georoc.mpch-mainz.gwdg.de/).

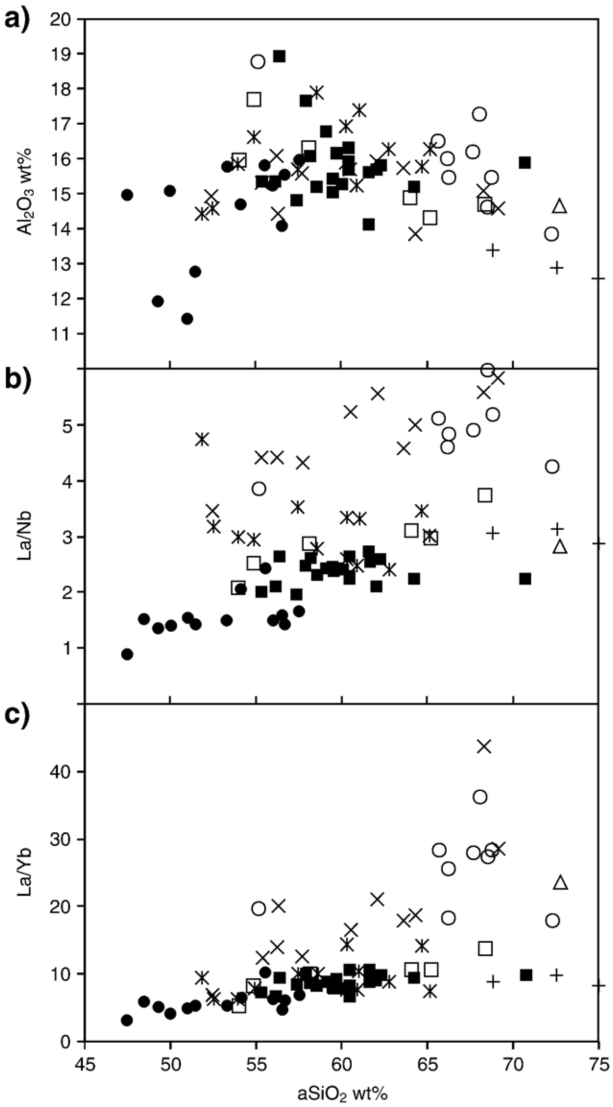

Fig. 6. Variation diagram showing Al_2O_3, La/Nb and La/Yb vs. SiO_2 (anhydrous) for trace element enriched basalt–dacite units of the Warrawoona Group (Pilbara Supergroup) (symbols as for Fig. 5). With decreasing age (Coonterunah→Duffer→Panorama), the rock groups become generally more silicic and have higher average La/Nb and La/Yb as a result of the presence of increasingly TTG-like rocks.

5.1. The Whundo Group

The Whundo Group is volumetrically dominated by basaltic to andesitic rocks and can be broadly divided geochemically into three packages (Fig. 8; Smithies et al., 2005a). The lower volcanic package is dominated by calc-alkaline basaltic to andesitic lavas but includes ~1–10-m-thick flow units with boninite-like compositions, which are interbedded throughout and form up to ~15% of the package. Tholeiitic lavas dominate the middle volcanic package, but rare flows of boninite-like lavas persist into the lower parts of this package and calc-alkaline basaltic to andesitic lavas are interleaved with tholeiites in the higher levels. The upper volcanic package contains abundant calc-alkaline basaltic to dacitic flows, including adakitic lavas, with minor flows of Nb-rich basalt and LREE-rich dacite near the top. Initial ε_{Nd} values for this group are only slightly more radiogenic than depleted mantle, indicating very little involvement of older felsic crust.

The boninite-like rocks (Table 1) have an average SiO_2 value of ~52.5 wt.% (anhydrous), MgO~9.0 wt.%, $Mg^{\#}$~63 and TiO_2~0.3 wt.%. Smithies et al. (2004a, 2005a) showed that LREE-enrichments in these rocks did not reflect assimilation of any locally or regionally available crust. Rather, the combination of low TiO_2, Gd/Yb and Yb/Sc, high Al_2O_3/TiO_2 and significant LREE-enrichments and HFSE-depletion (Fig. 9) point to a strongly refractory source that was re-enriched prior to, or during, remelting. In terms of all other critical compositional features (e.g. low TiO_2, high La/Gd, low Gd/Yb and Yb/Sc), the Whundo boninite-like rocks more closely match modern boninites than any other Archean rocks.

The three main stratigraphic levels of calc-alkaline basaltic to andesitic rocks show subtle geochemical distinctions but are typically depleted in HREE and are distinctly enriched in incompatible trace elements (Fig. 9), with La/Yb~5.2 and La/Nb~2.2 (Table 1). Like the boninites, Nb vs. La/Nb systematics in these rocks cannot be explained through mixing of average Archean crust, or average Pilbara crust (Smithies et al., 2005a). In the best-preserved calc-alkaline basaltic to andesitic unit, decreasing Cr, Ni and $Mg^{\#}$ and increasing HREE and HFSE concentrations are broadly correlated with decreasing La/Sm and La/Yb ratios. There is also a broad positive correlation between LILE concentration and Cr and La/Yb ratio (Fig. 10). Broad negative correlations also occur between LILE concentrations and HFSE and HREE (Fig. 7). These trends are opposite to those expected during decompression partial melting, fractional crystallisation or crustal assimilation. Similar paradoxical trends, however, are seen in modern arc and back-arc magmas and are interpreted to reflect flux melting, where a strong sympathetic tie exists between the extent of partial melting and the amount of introduced subduction-derived fluids (e.g. Taylor and Martinez, 2003; Gribble et al., 1996). If these calc-alkaline basaltic to andesitic rocks are indeed subduction related then strong negative correlations between Ba/Th (and Cs/Th) and HFSE and HREE (Fig. 10) suggest that fluid-mediated metasomatism was the major process. Systematic decreases in Ba/La ratios with increasing stratigraphic height, however, suggest an increasing slab-melt component. This, in turn, is consistent with the presence of adakites and then Nb-enriched basalts in the immediately overlying sequence, both of which require a source that was metasomatised by slab-melt (Martin et al., 2005 and references therein).

5.2. Basaltic rocks of the De Grey Supergroup

The age of basaltic rocks in the De Grey Supergroup can be constrained to between ~3.0 and 2.95 Ga. They are found in the Mallina and Goldsworthy Basins (Fig. 7), but typically form only a minor component. However, they are locally abundant within the Bookingarra Group, which forms the upper part of the Mallina Basin. The rocks are typically basalts or siliceous

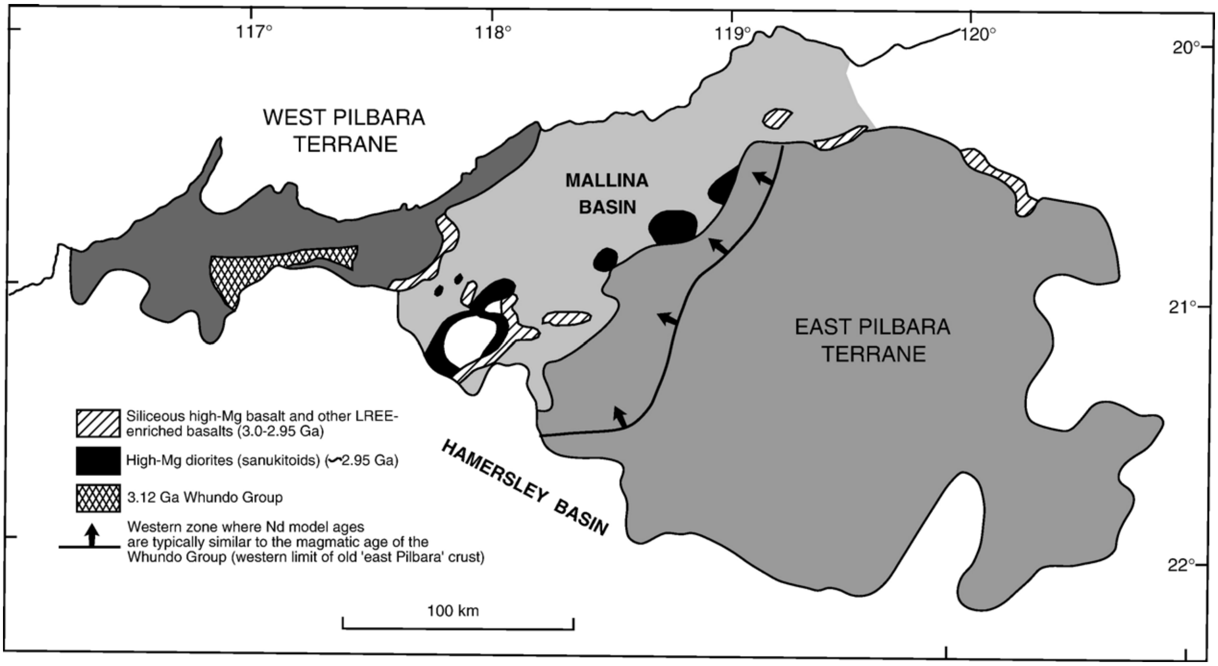

Fig. 7. Map showing the distribution of various subduction-enriched magmatic units of the West Pilbara Terrane and the Mallina Basin, as well as the western limit of 'old Pilbara crust' as defined by young (~3.12 Ga or younger) Nd depleted-mantle model ages (based on ~100 Nd isotopic analyses; Geological Survey of Western Australia and Geoscience Australia—unpublished data).

high-magnesian basalts (e.g. Sun et al., 1989) with SiO_2~55.5 wt.%, MgO~5.5 wt.% and $Mg^{\#}$~55. They are characterised by flat normalised HREE patterns but have significant enrichments in Th and LREE, with La/Yb~8.2 and La/Nb~3.2. They have non-radiogenic Nd-isotopic compositions ($\varepsilon_{Nd(2.95\,Ga)}$ mostly <−1.0). Within the Mallina Basin, three distinct stratigraphic units of these basalts and siliceous high-magnesian basalts occur, each with subtly different compositions (Smithies et al., 2004b). An additional suite of contemporaneous LREE-enriched gabbros intrude the sedimentary basin rocks, and also intrudes beyond the basin limits, occurring 50 km northwest of the basin in the Cleaverville area of the West Pilbara Terrane.

Also intruding the Mallina Basin between ~2.97 and 2.95 Ga, forming a subvolcanic sill, is another suite of boninite-like rocks. These rocks have SiO_2~52.6 wt.%, $Mg^{\#}$~66, TiO_2 <0.3 wt.% and high Al_2O_3/TiO_2 (62–74) and CaO/TiO_2 (29–31) (Table 1). They have strongly fractionated LREE and HREE patterns resulting in prominent 'U-shaped' trace element patterns (Fig. 9), but differ from the older boninites of the Whundo Group in having higher HREE and La/Yb and significantly lower Gd/Yb.

The strong enrichments in Th and LREE, and the non-radiogenic Nd-isotopic compositions of the basaltic rocks of the De Grey Supergroup clearly suggest the incorporation of a crustal component. Arndt et al. (2001) suggested that these rocks formed from komatiitic magmas that assimilated felsic crust—like siliceous high-magnesian basalts elsewhere (Arndt and Jenner, 1986; Barley, 1986; Sun et al., 1989). Smithies et al. (2004b), however, pointed out that while the basalts, boninite-like rocks and gabbro of the Mallina Basin and Cleaverville areas cover a combined geographical extent of at least 18 000 km^2 and have intruded through compositionally diverse crust, they have a remarkably narrow range in La/Nb (~3.1), La/Sm (~5.3), La/Zr (~0.15) and a relatively narrow range of $\varepsilon_{Nd(2.95\,Ga)}$ (−0.6 to −2.8). This compositional homogeneity is inconsistent with assimilation of felsic crust, particularly given the known heterogeneity of Pilbara crust (e.g. Smithies et al., 2004b).

Furthermore, geochemical modelling shows that the individual members of the Mallina mafic suite are unlikely to be related to each other by AFC-type processes because any viable crustal contaminant must not only have had a La/Sm ratio atypical of most of the exposed felsic rocks in the region (Fig. 11) but also a ratio that varied within a very narrow range (~5.3) over the regional geographic extent of the suite (Smithies et al., 2005b). Likewise, it is unlikely that assimilation of crust into magmas similar to those that formed the boninite-like rocks (the most primitive of the mafic suite), prior to closed system fractionation (perhaps in a series of higher level chambers), produced the evolved basaltic and gabbroic magmas. This is because some of the basalts have twice the concentration of Ni and three times the Th and LREE concentrations of the boninite-like rocks with similar $Mg^{\#}$. Additionally, La/Yb ratios in some basalts (up to ~12.5) are significantly higher than those of the boninite-like rocks (~3.5) and cannot be explained via fractionation of olivine and orthopyroxene, without removal also of clinopyroxene, which would have resulted in La/Zr and La/Sm ratios that were too high and too low respectively.

The Nd-isotopic composition of the Mallina mafic suite appears to be largely controlled by a mixture of non-radiogenic crust, similar to old Pilbara crust [i.e., >3.3 Ga, $\varepsilon_{Nd(2.95\,Ga)}$<−2.3, high La/Nb, (Sm, Zr)], and variably

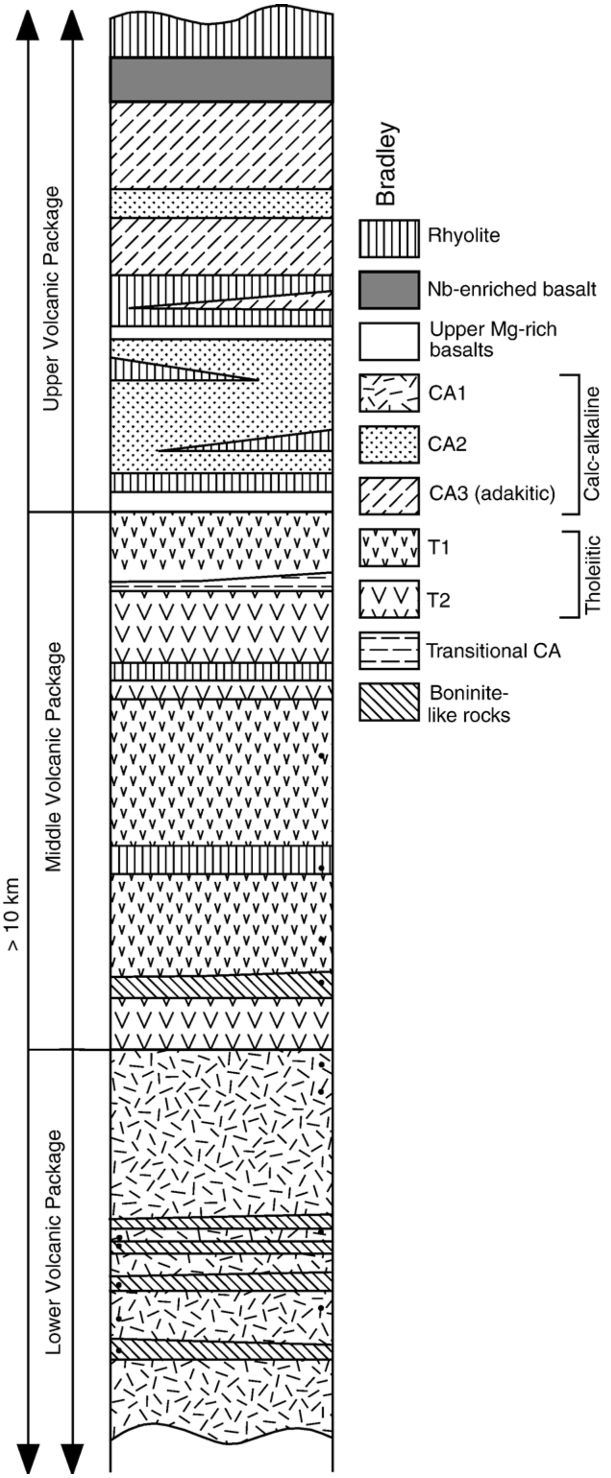

Fig. 8. Schematic stratigraphic section through the Whundo Group of the West Pilbara Terrane.

depleted (non-chondritic) mantle ($\varepsilon_{Nd(2.95\,Ga)}$>+1.0), quite possibly Whundo-like depleted crust [i.e., $\varepsilon_{Nd(2.95\,Ga)}$>−0.4, low La/Nb, (Sm, Zr)]. Despite this, the compositional homogeneity shown by the Mallina mafic suite requires that the crustal components were homogenised before incorporation into the magmas. Smithies et al. (2004b) suggested that the Mallina mafic suite was most likely derived from a mantle source that incorporated subducted sediment; in this case, a homogeneous mix of 'old-Pilbara crust' and crust that resembled c. 3.12 Ga greenstones of the Whundo Group which crop out to the northwest of the basin.

5.3. High-Mg diorites (sanukitoids)

An extensive high-Mg diorite (sanukitoid) suite forms a northeast-trending chain of high-level intrusions extending for over 150 km along the axis of the Mallina Basin (Smithies and Champion, 2000) (Fig. 7). These intrusions were emplaced into zones of active dilation related to extension along crustal-scale basin-parallel faults between 2.955 and 2.945 Ga.

The term "Archean sanukitoid suite" was first used by Shirey and Hanson (1984) to describe a suite of dioritic to granodioritic rocks, the more mafic of which (60 wt.% SiO_2 or less) have MgO > 6 wt.%, $Mg^{\#}$ > 60, Ni and Cr > 100 ppm, coupled with high LILE and Th, low HFSE (Fig. 4) and high Na_2O, K_2O, LREE and LREE/HREE (e.g. La/Yb ~ 7.8). They are a widespread, but minor (probably ≪5% of Archean granitic rocks) component of many Neoarchean terranes (Shirey and Hanson, 1984). The high-Mg diorite suite of the Mallina Basin is the oldest recognised example of this type of magmatism.

A mantle source component is required for the high-Mg diorite suite to explain the high $Mg^{\#}$ and high Cr and Ni concentrations (Shirey and Hanson, 1984), but even the most primitive diorites also show extreme enrichment in Th and LREE with no apparent correlation with either $Mg^{\#}$, ε_{Nd}, Cr, Ni or SiO_2. For the high-Mg diorite (sanukitoid) suite of the Mallina Basin, plutons with higher $Mg^{\#}$ (>55) and Cr (>150 ppm) often have amongst the highest SiO_2 (>66 wt.%), K_2O (up to 4 wt.%) and Th (up to 33 ppm), suggesting that the enrichment within the suite was not simply the result of crystal fractionation or crustal contamination. A significantly LILE-enriched mantle source is the most reasonable explanation for the composition of these rocks (e.g. Shirey and Hanson, 1984; Evans and Hanson, 1997; Smithies and Champion, 2000).

The high-Mg diorite suite is consistently and significantly more radiogenic than the basalts of the Mallina mafic suite, with ε_{Nd} values between −0.1 and +0.8, but with higher LREE concentrations and LREE/HREE ratios at similar $Mg^{\#}$. These features can be explained if, compared to the source for the Mallina mafic suite, the mantle source for the high-Mg diorites incorporated a crustal component with a considerably lower ratio of old Pilbara-like crust to basaltic Whundo-like crust, particularly if the enriched component is a high La/Yb adakitic melt derived through high-pressure (garnet-stable) melting of subducted mafic (Whundo-like) crust (Smithies et al., 2004b).

6. Subduction history of the Pilbara Craton

Geochemical evidence from basaltic rocks of the lower Pilbara Supergroup neither strongly implicates nor refutes a subduction origin. The hydrated basaltic source of TTG can

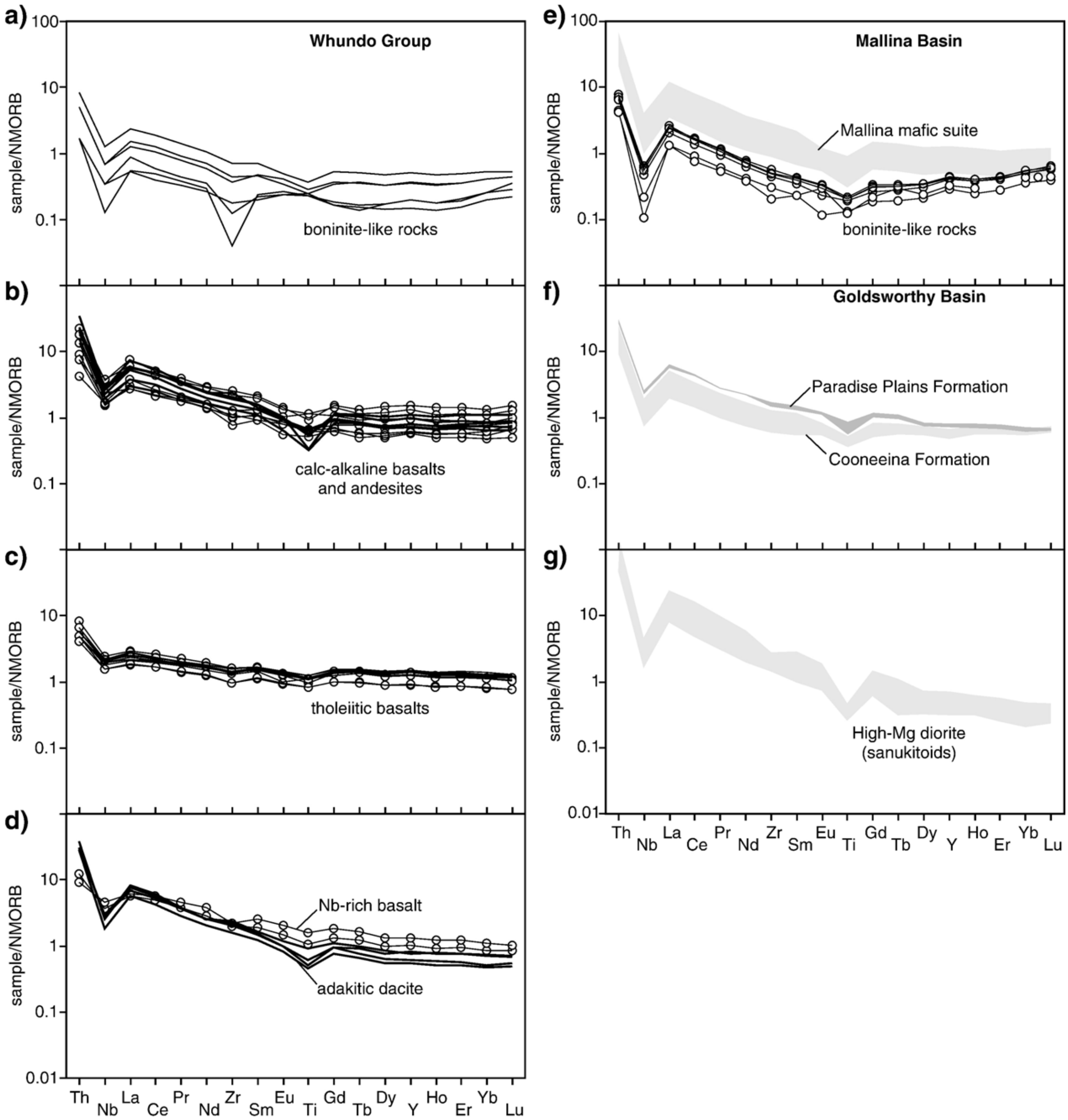

Fig. 9. Same as Fig. 3. MORB normalised trace element diagrams for magmatic units of the West Pilbara Terrane and of the Mallina Basin Pilbara Supergroup. (Normalising values from Sun and McDonough, 1989.)

been interpreted as both subducted mafic crust or thickened crust and so the contribution of TTG-like material to the felsic volcanism within the lower Pilbara Supergroup, as well as to contemporaneous intrusions, provides no direct evidence for subduction. Importantly, none of these TTG-like rocks have the high $Mg^{\#}$ characteristic of TTGs that have reacted with mantle wedge peridotite (e.g. Smithies, 2000; Martin and Moyen, 2002; Martin et al., 2005). If these rocks formed during subduction, it was likely to be very flat (Smithies et al., 2003; Martin et al., 2005). Some of the enriched volcanic series of the lower Pilbara Supergroup have features in common with Phanerozoic calc-alkaline rocks found in continental subduction settings. However, these 'enriched' packages are stratigraphically bound, above and below, by thick sequences of basalt with low La/Nb and La/Sm ratios and no evidence of having sampled any source compositionally resembling a modern mantle wedge. Furthermore, the geochemistry of some of the felsic series (e.g. C-F2, D-F1) is more consistent with fractionation of similar tholeiitic sequences, rather than with a calc-alkaline line of descent.

The voluminous basaltic rocks from the lower to upper part of the Pilbara Supergroup are derived from two sources; a plume source and a lithospheric mantle source (Smithies et al., 2005b). The relative contribution from each source does not appear to have changed with time and, although the lithospheric mantle

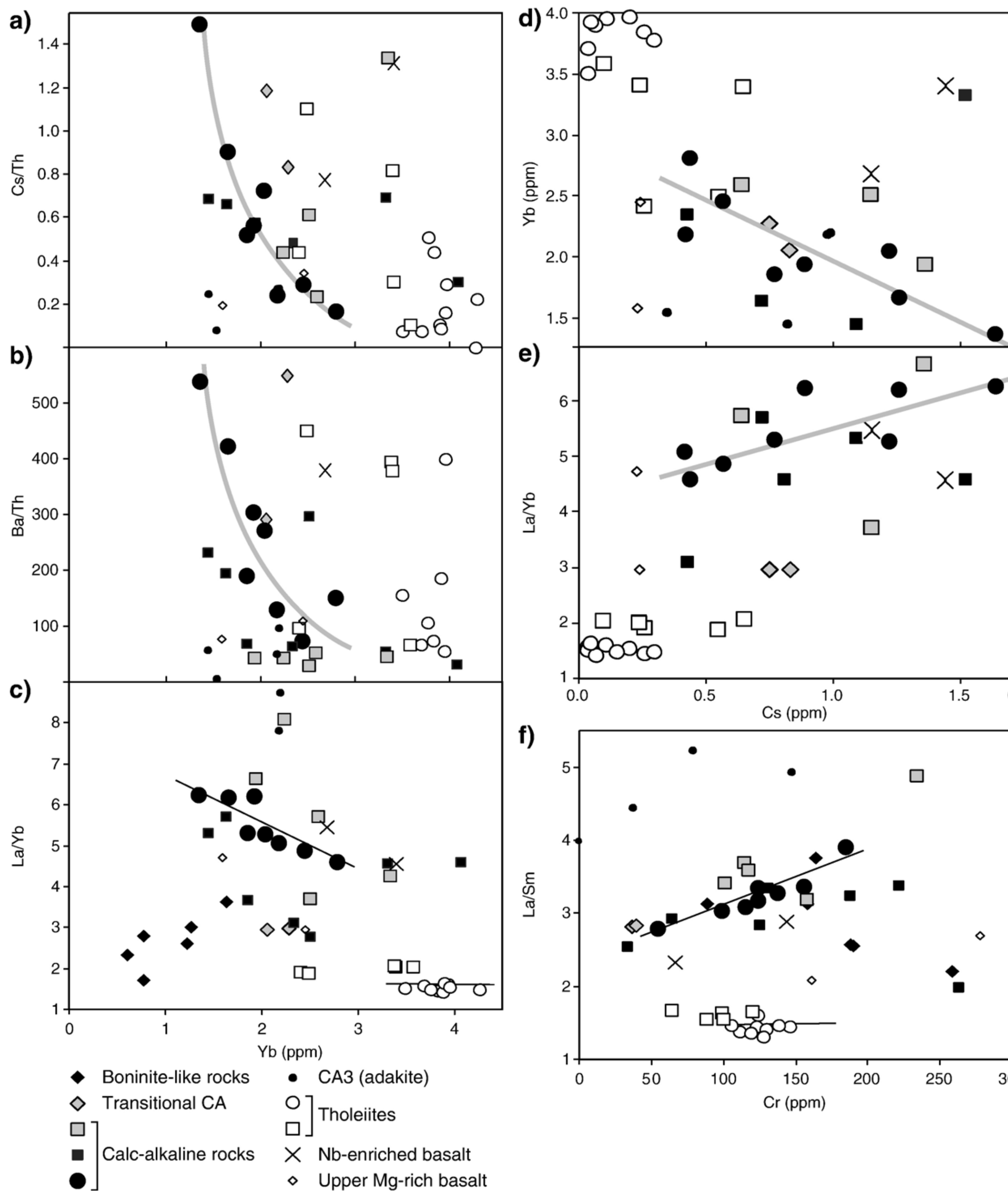

Fig. 10. Various trace element variation diagrams for the rocks of the Whundo Group of the West Pilbara Terrane (modified from Smithies et al., 2005a).

source does appear to have become more depleted over time, there is no fundamental change in the compositional range of the voluminous basaltic rocks with age. In contrast, the felsic volcanic units progressively evolve from tholeiitic to TTG-like to intra-crustal high-K melts over the same period. These trends are also consistent with isotopic trends and age patterns from granites of the East Pilbara Terrane (Champion and Smithies, 2001; Smithies et al., 2003). This suggests that the felsic component evolved independently of the mafic component as a result of the progressive recycling of pre-existing crust, without any need for the addition of significant juvenile material. This felsic trend occurred over an extraordinarily long time span (~300 my) across the East Pilbara Terrane.

Thus, the cyclic lithological architecture of the Pilbara Supergroup implies a repeating petrogenetic event which itself involves two fundamentally different but related processes—mantle melting, most likely related to mantle plumes, and crustal melting. Superimposed on this is a secular process with progressively younger lithological packages containing progressively more evolved ('crustal') felsic volcanics.

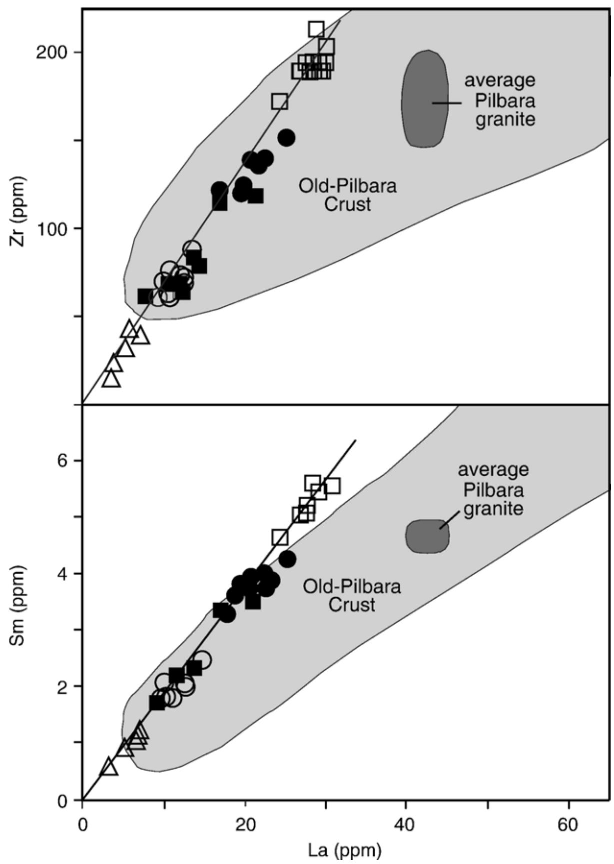

Fig. 11. Variation diagrams showing Zr and Sm vs. La for basalts of the Mallina Basin and comparing these to the fields for 'old-Pilbara crust' and average Pilbara granite (modified from Smithies et al., 2004b).

If these cycles–including the lower enriched felsic units–are a result of some form of subduction process, then they reflect an unusually thick series of stratigraphically superimposed, rather than tectonically accreted, subduction cycles and with only very limited stratigraphic intervals that show any evidence at all for mantle source metasomatism. If modern-styles of subduction occurred throughout the 3.51–3.2 Ga depositional period of the Pilbara Supergroup, then no clear evidence for it remains in the preserved rock record. We do not discount the possibility that some form of subduction occurred throughout this period–or even earlier–but we suggest that if it did, it shared very little in common with modern-style subduction processes and was more likely dominated by flat subduction (e.g. 'Archean flat subduction'—Smithies et al., 2003).

In contrast with the East Pilbara Terrane, the mainly younger tectonic units that comprise the West Pilbara Terrane and the basins that host the De Grey Supergroup preserve several strong lines of evidence that modern-style tectonic process operated, at least locally, by 3.12 Ga. The linear structural fabric of the terrane, the presence of lithologically and geochronologically exotic belts, and the presence of a broad belt of isotopically more juvenile crust are consistent with some form of convergent margin and are difficult to account for within any other tectonic context. The 3.12 to 2.95 Ga volcanic rocks show a dramatic shift in compositional style and in lithological diversity and association from the volcanic sequences preserved in the Pilbara Supergroup. They form a belt, flanking the northern and western margin of the old eastern cratonic nucleus (Fig. 7), of magmas derived from a variably depleted mantle source but that have enriched geochemical signatures that cannot be accounted for by crustal contamination.

It is hard to imagine that a modern-style subduction setting would be questioned for a Phanerozoic succession that matched the Whundo Group in terms of the composition of individual units and, more particularly, the overall lithological and geochemical architecture. The absence of clear evidence for basement material and of exotic "continental" sedimentary material is most consistent with an intraoceanic arc setting, and the low Th/La ratios (0.07 to 0.14), Ce/Yb (typically <40) and La/Nb ratios are characteristic of intraoceanic arc settings (e.g. Hawkesworth et al., 1993; Jolly et al., 2001). The Whundo Group likely represents Earth's oldest preserved intraoceanic arc, and this accreted to northwestern edge of the East Pilbara Terrane at some stage between 3.12 and 2.95 Ga.

The basins that host the De Grey Supergroup form a belt that overlies the suture marking the accretion of the Whundo Group. While there is no regional evidence for subduction contemporaneous with deposition of the De Grey Supergroup and associated mafic rocks, or with emplacement of the high-Mg diorite (sanukitoid) suite, the composition of these magmas points strongly to a highly enriched mantle source. The compositional homogeneity show by the Mallina mafic suite requires that the crustal components were homogenised before incorporation into the magmas and a mantle source that incorporated homogenised subducted sediment appears the most likely model. The enriched component in the mantle source for the Mallina mafic suite and for the high-Mg diorites can be modelled as contrasting mixtures of the same two crustal components; 'old-Pilbara crust' [i.e., >3.3 Ga, $\varepsilon_{Nd(2.95\,Ga)} < -2.3$, high La/Nb, (Sm, Zr)] and basaltic crust similar to the c. 3.12 Ga Whundo Group [$\varepsilon_{Nd(2.95\,Ga)} > -0.4$, low La/Nb, (Sm, Zr)] (Smithies et al., 2004b). We suggest that prior to, or during, accretion of the Whundo Group to the East Pilbara Terrane, c. 3.12 Ga Whundo mafic crust and homogeneous sediment derived from old (>3.3 Ga) Archean terranes was subducted to the southeast and that partial melts derived from the subducted sediments infiltrated the mantle wedge. Resulting metasomatism was homogeneous in regards to ratios involving LREE and Zr, at least over an area large enough to provide the source that later produced the Mallina mafic suite. The mantle source for the high-Mg diorite suite was metasomatised by a component with a high proportion of slab-melt (Smithies and Champion, 2000). This would explain the more radiogenic Nd-isotopic compositions and the higher LREE concentrations and LREE/HREE ratios of the high-Mg diorite suite, particularly if melting of the slab occurred at pressures high enough to stabilise garnet. We suggest that at greater depths, within the stability field of garnet, mafic Whundo-like crust itself partially melted to produce small volumes of adakitic magmas. These continuously interacted with mantle material (e.g. Kelemen, 1995; Rapp et al., 1999) as they ascended, but because of low melt/wall-rock ratios, froze (e.g. Rapp et al., 1999) close to the base of the lithosphere, where they provided the source for subsequent high-Mg diorite suite magmatism.

7. Discussion

The Archean rock record is commonly poorly preserved and fragmentary and rock relationships are consequently very poorly constrained. In such circumstances, the geochemistry of least-altered igneous rocks typically provides the only constraints on how crust and mantle have interacted, and is frequently used to infer a regional tectonic setting. Geochemical arguments alone, however, typically cannot prove or disprove the existence of a metasomatised mantle (wedge) source, and, by corollary, the likely operation of modern-style subduction processes. This is as true in the Phanerozoic as it is in the Archean, but the more holistic data set required to support any particular inferred tectonic setting becomes increasing difficult to acquire with increasingly old terranes. The Pilbara Craton, in northwestern Australia, is one of the best-preserved Archean terranes in the world, and one of the few to contain a rock record that spans from the Paleoarchean to the Neoarchean. If modern-style plate tectonic processes first emerged in the Archean, the Pilbara Craton likely provides the best laboratory to investigate this.

The Paleoarchean East Pilbara Terrane forms the ancient nucleus of the craton. Here, the geochemistry of the c. 3.52 Ga–3.25 Ga mafic and intermediate volcanic rocks indicates that the dominant crustal growth was, for the most part, via processes unlike those of modern subduction, and more like those expected in a plume environment. Within this package, there are a few stratigraphic horizons with geochemistry consistent with magmatism at modern-style subduction environments. These horizons, however, form only a minor part of the overall package, are stratigraphically bound between more voluminous 'plume-type' horizons, and have geochemical signatures that are equally consistent with such other processes as assimilation (and fractional crystallisation) of crust (likely TTG-like) into magmas similar to those that formed the surrounding tholeiitic basalts. Thus, the evidence for modern-style tectonic processes from the East Pilbara Terrane is at best inconclusive. But while the balance of evidence likely favours a plume-dominated system, it does not negate some form of subduction process during this period of time.

The West Pilbara Terrane contrasts strongly with the East Pilbara Terrane in terms of lithostratigraphy, geochemistry and tectonic style. The cumulative geological evidence from the West Pilbara Terrane and the basins that host the De Grey Supergroup, provides strong evidence for modern-style subduction processes. Here, there is a dramatic shift in compositional style and lithological diversity and association from the volcanic sequences preserved in the Pilbara Supergroup. These western volcanic sequences form a belt, flanking the northern and western margin of the old eastern cratonic nucleus, of magmas derived from a variably depleted mantle source coupled with enriched geochemical signatures that cannot be accounted for by crustal contamination. Importantly, the evidence for modern-style subduction processes in this region does not rely solely on geochemical arguments. It also derives from several independent pieces of geological evidence, including a linear magmatic and structural fabric, the presence of lithologically and geochronologically exotic greenstone belts, and the presence of a broad belt of isotopically more juvenile crust. The collective strength of these arguments is compelling—some form of convergent margin setting existed along the northwestern margin of the East Pilbara Terrane at 3.12 Ga, most likely an intra-oceanic (Whundo) arc. Later accretion of that terrane to the East Pilbara cratonic nucleus further added to the regionally metasomatised mantle source, which then produced the basalts of the De Grey Supergroup and the high-Mg diorite suite between 2.97 and 2.95 Ga.

The Mesoarchean assemblages that flank the East Pilbara Terrane show that plate tectonic processes operating in that region had acquired many of the attributes of those that characterise modern convergent margins. These assemblages mark the *minimum* age for the birth of modern-style plate subduction process.

Acknowledgements

We would like to express our great appreciation and thanks to Arthur Hickman for continuous encouragement and support and for endless fruitful discussions throughout the ~10 years he has managed the Geological Survey of Western Australia's Pilbara Mapping Program. Comments from A. Budd and journal reviews by Rob Kerrich and Ali Polat significantly improved the manuscript. Published with the permission of the Director, Geological Survey of Western Australia and the Chief Executive Officer, Geoscience Australia.

References

Abbott, D.H., Hoffman, S.E., 1984. Archaean plate tectonics revisited: 1. Heat flow, spreading rate, and the age of subducting lithosphere and their effects on the origin and evolution of continents. Tectonics 3, 429–448.

Arndt, N.T., Jenner, G.A., 1986. Crustally contaminated komatiites and basalts from Kambalda, Western Australia. Chemical Geology 56, 229–255.

Arndt, N., Bruzak, G., Reischmann, T., 2001. The oldest continental and oceanic plateaus: geochemistry of basalts and komatiites of the Pilbara Craton, Australia. In: Ernst, R.E., Buchan, K.L. (Eds.), Mantle Plumes: Their Identification Through Time. Special Paper - Geological Society of America, vol. 352, pp. 359–387.

Ayer, J., Amelin, Y., Corfu, F., Kamo, S., Ketchum, J., Kwok, K., Trowell, N., 2002. Evolution of the southern Abitibi greenstone belt based on U–Pb geochronology: autochthonous volcanic construction followed by plutonism, regional deformation and sedimentation. Precambrian Research 115, 63–95.

Barley, M.E., 1986. Incompatible-element enrichment in Archaean basalts: a consequence of contamination by older sialic crust rather than mantle heterogeneity. Geology 14, 947–950.

Barley, M.E., 1997. The Pilbara Craton. In: de Wit, M.J., Ashwal, J. (Eds.), Greenstone Belts. Oxford University Monographs on Geology and Geophysics, vol. 35. Clarendon Press, pp. 657–664.

Bickle, M.J., Morant, P., Bettenay, L.F., Boulter, C.A., Blake, T.S., Groves, D.I., 1985. Archaean tectonics of the Shaw Batholith, Pilbara Block, Western Australia: structural and metamorphic tests of the batholith concept. In: Ayers, L.D., Thurston, P.C., Card, K.D., Weber, W. (Eds.), Evolution of Archean Supracrustal Sequences. Special Paper - Geological Association of Canada, vol. 28, pp. 325–341.

Blewett, R.S., 2002. Archaean tectonic processes: a case for horizontal shortening in the North Pilbara granite-greenstone terrane, Western Australia. Precambrian Research 113, 87–120.

Boily, M., Dion, C., 2002. Geochemistry of boninite-type volcanic rocks in the Frotet-Evans greenstone belt, Opatica subprovince, Quebec: implications for the evolution of Archaean greenstone belts. Precambrian Research 115, 349–371.

Brauhart, C., 1999. Regional alteration systems associated with Archean volcanogenic massive sulphide deposits at Panorama, Pilbara, Western Australia: Unpublished PhD thesis, University of Western Australia, 194 pp.

Buick, R., Brauhart, C.W., Morant, P., Thornett, J.R., Maniw, J.G., Archibald, N.J., Doepel, M.G., Fletcher, I.R., Pickard, A.L., Smith, J.B., Barley, M.E., McNaughton, N.J., Groves, D.I., 2002. Geochronology and stratigraphic relationships of the Sulphur Springs Group and Strelley Granite: a temporally distinct igneous province in the Archaean Pilbara Craton, Australia. Precambrian Research 114, 87–120.

Burke, K., Dewey, J.F., Kidd, W.S.F., 1976. Dominance of horizontal movements, arc and microcontinent collision during the later permobile regime. In: Windley, B.F. (Ed.), The Early History of the Earth. Wiley, London, pp. 113–129.

Champion, D.C., Smithies, R.H., 2001. Archaean granites of the Yilgarn and Pilbara cratons, Western Australia. In: Cassidy, K.F., Dunphy, J.M., Van Kranendonk, M.J. (Eds.), 4th International Archaean Symposium 2002, Extended Abstracts,. AGSO-Geoscience Australia, Record 2001/37, pp. 134–136.

Collins, W.J., 1993. Melting of Archaean sialic crust under high a_{H_2O} conditions: genesis of 3300 Ma Na-rich granitoids in the Mount Edgar Batholith, Pilbara Block, Western Australia. Precambrian Research 60, 151–174.

Condie, K.C., 2005. High field strength element ratios in Archean basalts: a window to evolving sources of mantle plumes? Lithos 79, 491–504.

Cullers, R.L., DiMarco, M.J., Lowe, D.R., Stone, J., 1993. Geochemistry of a silicified, felsic volcaniclastic suite from the early Archaean Panorama Formation, Pilbara Block, Western Australia: an evaluation of depositional and post-depositional processes with a special emphasis on the rare-earth elements. Precambrian Research 60, 99–116.

Davies, G.F., 1992. On the emergence of plate tectonics. Geology 20, 963–966.

Davies, G.F., 1993. Conjectures on the thermal and tectonic evolution of the Earth. Lithos 30, 281–289.

Davies, G.F., 1998. Plates, plumes, mantle convection, and mantle evolution. In: Jackson, I. (Ed.), The Earth's Mantle. Cambridge University Press, pp. 228–258.

Evans, O.C., Hanson, G.N., 1997. Late- to post-kinematic Archean granitoids of the S.W. Superior Province: derivation through direct mantle melting. In: de Wit, M., Ashwal, J. (Eds.), Greenstone Belts. Oxford University Press, Oxford, pp. 280–295.

Glikson, A.Y., Davy, R., Hickman, A.H., Pride, C., Jahn, B., 1987. Trace elements geochemistry and petrogenesis of Archaean felsic igneous units, Pilbara Block, Western AustraliaBureau of Mineral Resources, Record 1987/30. 63 pp.

Gribble, R.F., Stern, R.J., Bloomer, S.H., Stuben, D., O'Hearn, T., Newman, S., 1996. MORB mantle and subduction components interact to generate basalts in the southern Mariana Trough back-arc basin. Geochimica et Cosmochimica Acta 60 (12), 2153–2166.

Hamilton, W.B., 1998. Archean magmatism and deformation were not products of plate tectonics. Precambrian Research 91, 143–180.

Hamilton, W.B., 2003. An alternative earth. GSA Today 13, 4–12.

Hawkesworth, C.J., Gallagher, K., Hergt, J.M., McDermott, F., 1993. Mantle and slab contributions in arc magmas. Annual Review of Earth and Planetary Sciences 21, 175–204.

Hickman, A.H., 1983. Geology of the Pilbara Block and its environs. Bulletin - Geological Survey of Western Australia, vol. 127. 268 pp.

Hickman, A.H., 1997. A revision of the stratigraphy of Archaean greenstone successions in the Roebourne-Whundo area–west Pilbara. Western Australia Geological Survey, Annual Review 1996–97 76–81.

Hickman, A.H., 2004. Two contrasting granite-greenstones terranes in the Pilbara Craton, Australia: evidence for vertical and horizontal tectonic regimes prior to 2900 Ma. Precambrian Research 131 (3–4), 153–172.

Hickman, A.H., Van Kranendonk, M.J., 2004. Diapiric processes in the formation of Archaean continental crust, East Pilbara Granite-Greenstone Terrane, Australia. In: Eriksson, P.G., Altermann, W., Nelson, D.R., Mueller, W.U., Catuneau, O. (Eds.), The Precambrian Earth: Tempos and Events. Elsevier, pp. 54–75.

Hollings, P., Kerrich, R., 2000. An Archean arc basalt-Nb-enriched basalt–adakite association: the 2.7 Ga confederation assemblage of the Birch-Uchi greenstone belt, Superior Province. Contributions to Mineralogy and Petrology 139, 208–226.

Jahn, Bor-Ming, Gliksoon, A.Y., Peucat, J.J., Hickman, A.H., 1981. REE geochemistry of Archean silicic volcanics and granitoids from the Pilbara Block, Western Australia: implications for the early crustal evolution. Geochimica et Cosmochimica Acta 45, 1633–1652.

Jolly, W.A., Lidiak, E.G., Dickin, A.P., Wu, T.-W., 2001. Secular geochemistry of Central Puerto Rican Island arc lavas: constraints on Mesozoic tectonism in the Eastern Greater Antilles. Journal of Petrology 42/12, 2197–2214.

Kelemen, P.B., 1995. Genesis of high Mg andesites and the continental crust. Contributions to Mineralogy and Petrology 120, 1–19.

Kloppenburg, A., White, S.H., Zegers, T.E., 2001. Structural evolution of the Warrawoona greenstone belt and adjoining granitoid complexes, Pilbara craton, Australia, implications for Archean tectonic processes. Precambrian Research 112, 107–147.

Krapez, B., 1993. Sequence stratigraphy of the Archaean supracrustal belts of the Pilbara Block, Western Australia. Precambrian Research 60, 1–45.

Krapez, B., Eisenlohr, B., 1998. Tectonic settings of Archaean (3325–2775 Ma) crustal–supracrustal belts in the West Pilbara Block. Precambrian Research 88, 173–205.

Kröner, A., 1981. Precambrian plate tectonics. In: Kroner, A. (Ed.), Precambrian Plate Tectonics. Elsevier, pp. 57–90.

Manikyamba, C., Naqvi, S.M., Rao, D.V.S., Mohan, M.R., Khanna, T.C., Rao, T.G., Reddy, G.L.N., 2005. Boninites from the Neoarchean Gadwal Greenstone belt, Eastern Dharwar Craton, India: implications for Archean subduction processes. Earth and Planetary Science Letters 230, 65–83.

Martin, H., Moyen, J.-P., 2002. Secular changes in tonalite–trondhjemite–granodiorite composition as markers of the progressive cooling of Earth. Geology 30, 319–322.

Martin, H., Smithies, R.H., Rapp, R., Moyen, J.-F., Champion, D., 2005. An overview of adakite, tonalite–trondhjemite–granodiorite (TTG) and sanukitoid: relationships and some implications for crustal evolution. Lithos 79, 1–24.

McCall, G.J.H., 2003. A critique of the analogy between Archaean and Phanerozoic tectonics based on regional mapping of the Mesozoic–Cenozoic plate convergence zone in the Makran, Iran. Precambrian Research 127, 5–18.

Nisbet, E.G., Cheadle, M.J., Arndt, N.T., Bickle, M.J., 1993. Constraining the potential temperature of the Archaean mantle: a review of the evidence from komatiites. Lithos 30, 291–307.

Parman, S.W., Grove, T.L., Dann, J.C., 2001. The production of Barberton komatiites in an Archean subduction zone. Geophysical Research Letters 28, 2513–2516.

Pike, G., 2001. The facies architecture of two contrasting volcano-sedimentary basin successions from the Archaean Whim Creek Belt, North Pilbara Terrain, Western Australia: the intra-continental arc-related Whim Creek Group and plume-related, continental rift-hosted Bookingarra Group, Unpublished PhD thesis, Monash University. 465 pp.

Pike, G., Cas, R.A.F., 2002. Stratigraphic evolution of Archaean volcanic rock-dominated rift basins from the Whim Creek Belt, west Pilbara Craton, Western Australia. Special Publication of the International Association of Sedimentologists 33, 213–234.

Polat, A., Kerrich, R., 2006. Reading the geochemical fingerprints of Archean Hot subduction volcanic rocks: evidence for accretion and crustal recycling in a mobile tectonic regime. Geophysical Monograph Series, vol. 164. American Geophysical Union, pp. 189–213.

Polat, A., Hofmann, A.W., Rosing, M.T., 2002. Boninite-like volcanic rocks in the 3.7–3.8 Ga Isua greenstone belt, West Greenland: geochemical evidence for intra-oceanic subduction zone processes in the early Earth. Chemical Geology 184, 231–254.

Rapp, P.R., Shimizu, N., Norman, M.D., Applegate, G.S., 1999. Reaction between slab-derived melts and peridotite in the mantle wedge: experimental constraints at 3.8 GPa. Chemical Geology 160, 335–356.

Sandeman, H.A., Hanmer, S., Davis, W.J., Ryan, T.D., Peterson, T.D., 2004. Neoarchaean volcanic rocks, Central Hearne supracrustal belt, Western Churchill Province, Canada: geochemical and isotopic evidence supporting intra-oceanic, supra-subduction zone extension. Precambrian Research 134, 113–141.

Scott, D.J., St-Onge, M.R., Lucas, S.B., Helmstaedt, H., 1991. Geology and geochemistry of the Early Proterozoic Purtuniq ophiolite, Cape Smith Belt, northern Quebec, Canada. In: Peters, T.J., et al. (Ed.), Ophiolite Genesis and Evolution of the Oceanic Lithosphere. Ministry of Petroleum and Minerals, Sultanate of Oman, pp. 817–849.

Shchipansky, A.A, Samsonov, A.V., Bibikova, E.V., Babarina, I.I., Konilov, A.N., Krylov, K.A., Slabunov, A.I., Bogina, M.M., 2004. 2.8 Ga boninite-hosting partial subduction zone ophiolite sequences from the North Karelian greenstone belt, NE Baltic Shield, Russia. In: Kusky, T.M. (Ed.), Precambrian Ophiolites and Related Rocks. Elsevier, Amsterdam, pp. 425–486.

Shirey, S.B., Hanson, G.N., 1984. Mantle-derived Archaean monzodiorites and trachyandesites. Nature 310, 222–224.

Smith, J.B., Barley, M.E., Groves, D.I., Krapez, B., McNaughton, N.J., Bickle, M.J., Chapman, H.J., 1998. The Sholl Shear Zone, West Pilbara: evidence for a domain boundary structure from integrated tectonic analyses, SHRIMP U–Pb dating and isotopic and geochemical data of granitoids. Precambrian Research 88, 143–171.

Smithies, R.H., 2000. The Archaean tonalite–trondhjemite–granodiorite (TTG) series is not an analogue of Cenozoic adakite. Earth and Planetary Science Letters 182, 115–125.

Smithies, R.H., 2002. Archaean boninite-like rocks in an intracratonic setting. Earth and Planetary Science Letters 197, 19–34.

Smithies, R.H., Champion, D.C., 2000. The Archaean high-Mg diorite suite: links to tonalite–trondhjemite–granodiorite magmatism and implications for early Archaean crustal growth. Journal of Petrology 41, 1653–1671.

Smithies, R.H., Nelson, D.R., Pike, G., 2001. Development of the Archaean Mallina Basin, Pilbara Craton, northwestern Australia; a study of detrital and inherited zircon ages. Sedimentary Geology 141–142, 79–94.

Smithies, R.H., Champion, D.C., Cassidy, K.F., 2003. Formation of earth's early Archaean continental crust. Precambrian Research 127, 89–101.

Smithies, R.H., Champion, D.C., Sun, S-.S., 2004a. The case for Archaean boninites. Contributions to Mineralogy and Petrology 147, 705–721.

Smithies, R.H., Champion, D.C., Sun, S-.S., 2004b. Early evidence for LILE-enriched mantle source regions: diverse magmas from the c. 3.0 Ga Mallina Basin, Pilbara Craton, NW Australia. Journal of Petrology 45, 1515–1537.

Smithies, R.H., Champion, D.C., Van Kranendonk, M.J., Howard, H.M., Hickman, A.H., 2005a. Modern-style subduction processes in the Mesoarchaean: geochemical evidence from the 3.12 Ga Whundo intraoceanic arc. Earth and Planetary Science Letters 231, 221–237.

Smithies, R.H., Van Kranendonk, M.J., Champion, D.C., 2005b. It started with a plume—early Archaean basaltic proto-continental crust. Earth and Planetary Science Letters 238 (3–4), 284–297.

Stern, R.J., 2005. Evidence from ophiolites, blueschists, and ultrahigh-pressure metamorphic terranes that the modern episode of subduction tectonics began in Neoproterozoic time. Geology 33, 557–560.

Sun, S-.S., Hickman, H.H., 1999. Geochemical characteristics of ca 3.0 Ga Cleaverville greenstones and later mafic dykes, west Pilbara: implications for Archaean crustal accretionAustralian National University Research School of Earth Sciences Annual Report.

Sun, S-S., McDonough, W.F., 1989. Chemical and isotopic systematics of oceanic basalts: implications for mantle compositions and processes. In: Saunders, A.D., Norry, M.J. (Eds.), Magmatism in Ocean Basins. Special Publication - Geological Society of London, vol. 42, pp. 313–345.

Sun, S.-S., Nesbitt, R.W., McCulloch, M.T., 1989. Geochemistry and petrogenesis of Archaean and early Proterozoic siliceous high-magnesian basalts. In: Crawford, A.J. (Ed.), Boninites. Unwin Hyman, London, pp. 149–173.

Taylor, B., Martinez, F., 2003. Back-arc basin basalt systematics. Earth and Planetary Science Letters 210, 481–497.

Tomlinson, K.Y., Stott, G.M., Percival, J.A., Stone, D., 2003. Basement terrane correlations and crustal recycling in the western Superior Province: Nd isotopic character of granitoid and felsic volcanic rocks in the Wabigoon subprovince, N. Ontario, Canada. Precambrian Research 132, 245–274.

Van Kranendonk, M.J., 2004. Archaean tectonics 2004. A review. Precambrian Research 131, 143–151.

Van Kranendonk, M.J., Pirajno, F., 2004. Geological setting and geochemistry of metabasalts and alteration zones associated with hydrothermal chert ± barite deposits in the ca. 3.45 Ga Warrawoona Group, Pilbara Craton, Australia. Geochemistry: Exploration, Environment, Analysis 4, 253–278.

Van Kranendonk, M.J., Hickman, A.H., Smithies, R.H., Nelson, D.N., Pike, G., 2002. Geology and tectonic evolution of the Archaean North Pilbara terrain, Pilbara Craton, Western Australia. Economic Geology 97 (4), 695–732.

Van Kranendonk, M.J., Collins, W.J., Hickman, A.H., Pawley, M.J., 2004. Critical tests of vertical vs horizontal tectonic models for the Archaean East Pilbara Granite-Greenstone Terrane, Pilbara Craton, Western Australia. Precambrian Research 131, 173–211.

Van Kranendonk, M.J., Hickman, A. H., Smithies, R. H., Williams, I.R., Bagas, L., Farrell, T.R., in preparation. Revised lithostratigraphy of Archaean supracrustal and intrusive rocks in the northern Pilbara Craton, Western Australia. Western Australia Geological Survey, Record 2006/x.

Wilde, S.A., Valley, J.W., Peck, W.H., Graham, C.M., 2001. Evidence from detrital zircons for the existence of continental crust and oceans on the Earth 4.4 Gyr ago. Nature 409, 175–178.

Wyman, D.A., Kerrich, R., Polat, A., 2002. Assembly of Archean cratonic mantle lithosphere and crust: plume–arc interaction in the Abitibi-Wawa subduction–accretion complex. Precambrian Research 115, 37–62.

Zegers, T.E., Nelson, D.R., Wijbrans, J.R., White, S.H., 2001. SHRIMP U–Pb zircon dating of Archaean core complex formation and pancratonic strike-slip deformation in the East Pilbara Granite-Greenstone Terrain. Tectonics 20, 883–908.